Journal of Quantitative Spectroscopy & Radiative Transfer 291 (2022) 108344

Contents lists available at ScienceDirect

Journal of Quantitative Spectroscopy & Radiative Transfer

journal homepage: www.elsevier.com/locate/jqsrt

Diverging and converging schemes of approximations to describe fundamental EM Gaussian beams beyond the paraxial approximation

Gérard Gouesbet [a,*], Jianqi Shen [b], Leonardo A. Ambrosio [c]

[a] CORIA-UMR 6614- Normandie Université CNRS-Université et INSA de Rouen Campus Universitaire du Madrillet 76800, Saint-Etienne-du Rouvray, France
[b] College of Science, University of Shanghai for Science and Technology, 516, Jungong Road, Shanghai, 200093, China
[c] Department of Electrical and Computer Engineering São Carlos School of Engineering, University of São Paulo, 400 Trabalhador são-carlense Ave., São Paulo, SP 13566-590, Brazil

ARTICLE INFO

Article history:
Received 20 March 2022
Revised 21 July 2022
Accepted 14 August 2022
Available online 18 August 2022

Keywords:
Gaussian beams
Davis scheme of approximations
Standard beams
Localized approximations
Light scattering
Asymptotic series
Quantum electrodynamics

ABSTRACT

EM Gaussian beams are the most celebrated and used kind of laser beams. Their description beyond paraxial regimes has a long and venerable history, culminating may be with the building of a scheme of approximations which can be named the Davis scheme of approximations whose convergence has been considered as granted. Strange as it may be, a paper by Wang and Webb demonstrated that, actually, the Davis scheme is divergent. This quite unexpected result has been dramatically overlooked. This is the motivation for the present paper which reviews diverging and converging schemes of approximations to describe fundamental EM Gaussian beams. One of the new results obtained in the present framework is that a scheme of approximations known as the improved standard scheme, introduced more than two decades ago, is diverging as well. These divergences are the result of the behavior of asymptotic series similar to the ones encountered in quantum electrodynamics.

1. Introduction

Since its advent in 1960, thanks to both Théodore Maiman and a ruby crystal, the laser beam has become a very popular tool for various investigations, particularly using its most simple and ubiquitous version celebrated under the name of Gaussian beam. Such beams have been used in the field of light scattering. In particular, the GLMT which describes the interaction between arbitrary shaped beams and homogeneous spheres characterized by their diameter and their complex refractive index has originally been focused on the use of Gaussian beams, e.g. [1,2] although it is actually valid for any kind of laser beams [3,4]. Review papers devoted to GLMT, and more generally to T-matrix methods [5–8], allow one to gather a huge number of examples in which Gaussian beams have been used, e.g. [9–12] and references therein. Although it is not possible any more to extensively quote all papers dealing with Gaussian beams, let us however take the risk to name only a few papers associated with only a few topics, without explicitly taking into account the fact that some papers may pertain to several topics, with apologies to authors who should feel that they are unduly omitted.

A way to make an objective selection among the huge number of references available is, in order to limit the size of the room devoted to a review, to only retain those which use the word "Gaussian" in their title (except for a few motivated exceptions). We may then mention the issue of light scattering by particles of various shapes and morphologies, including homogeneous spheres [1,13–29], coated and multilayered spheres [30–34], particles with anisotropy properties [35–40], or with chiral properties [41,42], infinite cylinders of circular [43–63], and elliptical cross-sections [64,65], spheroids [66–76], assemblies of spheres and aggregates [77–82], various particles with various kinds of inclusions [83–89], slabs [90–92], or the case of a particle over a plane surface [93], see as well [94–96] for reviews, [97–99] for algorithmic discussions, [100] for the case of large particles, and [101–103] for miscellaneous cases.

Another important issue is the one devoted to the mechanical effects of light, made famous by Ashkin's work [104], with a recent review devoted to GLMTs [105]. They concern in particular the evaluation and the use of optical forces [106–112], and/or torques [113–119], optical levitation, traps and optical tweezers [120–127], binding phenomena [128,129], and stretching, stressing and deforming particles [130,131]. Another important field is the one of optical particle characterization using different measurement techniques such as velocimetry laser [132] and phase-Doppler techniques [133–136], microscopy [137], rainbow refractometry (corre-

* Corresponding author.
E-mail address: gouesbet@coria.fr (G. Gouesbet).

https://doi.org/10.1016/j.jqsrt.2022.108344
0022-4073/

lated with rainbow analysis) [138–145], holography [146,147], extinction techniques (correlated with extinction analysis) [148–150], or others such as in [151]. Other issues concern the study of resonances (Fano resonances, whispering gallery modes/morphology-dependent resonances) [106,152–156], photonic nanojets [157–159], and the validity of the optical theorem [160,161].

The above sample only provides a tiny amount of quotations of papers devoted to the description or to the use of Gaussian beams which are indeed the most popular kind of beams used. A good theoretical description of a fundamental Gaussian beam (mode TEM_{00}) is therefore of interest. It is only in 1979 that Davis proposed a scheme of approximations which would allow one to reach a description of Gaussian beams which, for a long time, has been supposed to be perfect [162], and therefore have indeed been used, in a form or in another, in several papers such as in [86,95,126,163–174]. The reader may be surprised by the large delay between the time of publication (1979) of the Davis scheme and the date (2012) of the first paper in the previous list. This is mainly due to an increasing interest with numerical techniques to solve Maxwell's equations in which the incident fields may be expressed in terms of coordinates. This should not obscure the fact that the Davis scheme has however been used in GLMT, in which the incident field is described in terms of beam shape coefficients (BSCs), as soon as 1985 [1]. It has furthermore be the source of the definition of standard beams (Sections Section 3, 4 and 5) and allowed a justification of the localized approximations to the evaluation of BSCs, associated with localized beam models (Section 4 and 5). It should be however noted that, whatever the refinement in the theoretical description of a beam, the experimental implementation of the intended beam may be far from being perfect, e.g. [19], a fact which has been a motivation for studying the possibility to measure the BSCs in the laboratory [175–178].

After all the successful implementations of the Davis scheme of approximations to the description of fundamental Gaussian beams, it is a huge unexpected result which told us that this scheme is actually divergent, as demonstrated in a much overlooked paper dated 2008 [179]. This result is the motivation for the present paper. After a short review on Gaussian beams provided above, we shall now discuss divergent and convergent schemes of description of Gaussian beams.

The paper is organized as follows. Section 2 deals with the Davis scheme and its divergence. Section 3 introduces a divergent version of what is known as standard beams. Section 4 deals with an improved standard scheme whose convergence seems to be guaranteed (an expectation later to be deceived), and with the convergent localized approximations (associated with localized beam models). Section 5 deals with numerical results, comparing intensity profiles obtained in the framework of GLMT, with BSCs expressed either by using a localized approximation or by using the improved standard beam description, and leading to the conclusion that the improved standard scheme is indeed divergent. These profiles are compared as well with the one of an ideal intended Gaussian beam profile. Section 6 deals with a complementary discussion, particularly concerning the fact that the divergent schemes discussed in the paper are the result of asymptotic series behavior made famous in the framework of quantum electrodynamics (QED), while Section 7 is a conclusion.

2. The Davis scheme and its divergence

2.1. The Davis scheme

To introduce the Davis scheme of approximations [162], completed by Barton and Alexander [180], Schaub et al. [181], let us consider a Gaussian beam with a time-dependence of the form $\exp(i\omega t)$ which propagates along the axis z' from negative to positive z', e.g. Fig. 1 reproduced from Gouesbet et al. [182]. Two parallel Cartesian coordinate systems, namely (x', y', z') and (x, y, z), are used to describe the configuration in hand, with (x', y', z') attached to the Gaussian beam and (x, y, z) used to describe the partial wave expansion of the beam. The origin of the beam system (x', y', z') is located at the center of the beam waist, and has a coordinate z_0 with respect to (x, y, z).

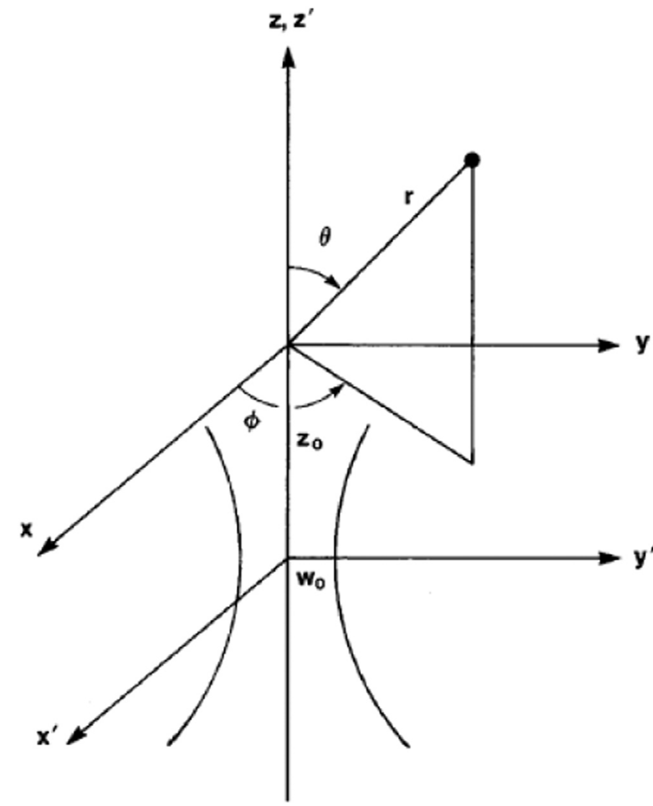

Fig. 1. Coordinate systems.

The story may then start with what is known as the solving paradox discussed by Lax et al. [183]. This paradox arises when we express the electric field of a Gaussian beam in the polarized form $\mathbf{E} = (E_{x'}, 0, 0)$ and assume that $E_{x'}$ is coordinate dependent. Maxwell's equation div $\mathbf{E}$ =0 then implies $\partial E_{x'}/\partial x' = 0$ which is in contradiction with the fact that we might have expected a Gaussian function to describe the functional dependence of $E_{x'}$ versus x'. Conversely, if we assume a Gaussian dependence of $E_{x'}$ versus x', then Maxwell's equations are not satisfied. To deal with this paradox, Lax et al. [183] examined a paraxial approximation and developed a perturbation procedure to systematically introduce higher-order corrections. Solutions of Maxwell's equations describing Gaussian beams are then expressed using expansions over successive powers of a small dimensionless parameter s which may be called the beam confinement factor (or beam shape factor) and is defined as:

$$s = w_0/l = 1/(kw_0) \tag{1}$$

in which w_0 is the beam waist radius and l is known as the diffraction length. Relying on this work and on an angular spectrum decomposition, Agrawal and Pattanyak [184] developed a somewhat similar approach, but restricted to solutions of the scalar (not vector) wave equation, and criticized by Seshadri [185] on the ground that their $(m = 1)$- first-order nonparaxial approximation does not have a correct asymptotic state. Rather than the approach by Lax et al., we shall expound an equivalent formulation due to Davis [162], see as well [182], which we favour because the introduction of a transversely polarized vector potential leads to a theory which is simpler and more appealing.

The potential vector is then written as:

$$\mathbf{A} = (A_x, 0, 0) \tag{2}$$

in which the non-zero component A_x is written as:

$$A_x = \psi(x, y, z)\exp(-ikz) \tag{3}$$

in which k is the wavenumber of the beam, and ψ a function which is not related to the Ricatti-Bessel function ψ_n of Eq. (99). The transverse coordinates x and y scale with a small transverse characteristic length, namely w_0, while the longitudinal coordinate z scales with a large longitudinal characteristic length, namely l. We then introduce rescaled coordinates according to:

$$\xi = \frac{x}{w_0},\ \eta = \frac{y}{w_0},\ \zeta = \frac{z}{l} \tag{4}$$

so that the derivatives $\partial\psi/\partial\xi$, $\partial\psi/\partial\eta$ and $\partial\psi/\partial\zeta$ now possess the same order of magnitude.

Within the Lorenz gauge, the vector potential $\mathbf{A}$ satisfies the Helmholtz equation:

$$\nabla^2\mathbf{A} + k^2\mathbf{A} = 0 \tag{5}$$

Inserting Eq. (3) into Eq. (5), we obtain a differential equation for ψ reading as:

$$\left(\frac{\partial^2}{\partial\xi^2} + \frac{\partial^2}{\partial\eta^2} - 2i\frac{\partial}{\partial\zeta} + s^2\frac{\partial^2}{\partial\zeta^2}\right)\psi = 0 \tag{6}$$

The function ψ is then expanded in powers of s^2 according to:

$$\psi = \sum_{n=0}^{\infty} s^{2n}\psi_{2n} = \psi_0 + s^2\psi_2 + s^4\psi_4 + \ldots \tag{7}$$

The lowest-order term ψ_0 represents the fundamental mode of the Gaussian beam, and is called the first-order Davis beam. As can be checked by use of Eq. (6), this mode reads as:

$$\psi_0 = iQ\exp[-iQ(\xi^2 + \eta^2)] \tag{8}$$

$$Q = \frac{1}{i + 2\zeta} \tag{9}$$

in which we have conveniently set $z_0 = 0$, so that (x', y', z') is changed to (x, y, z). Afterward, from ψ_0, we may recursively determine the higher-order modes for $n \geqslant 1$ using Eq. (6). Only ψ_2, named the third order mode, and ψ_4, named the fifth order mode, have been explicitly known thanks to [180], to be completed by a symmetric seventh order mode in 2002 [186] and by a symmetric ninth order mode in 2013 [126]. However, once an approximation to ψ is known, we may derive the corresponding expressions for the electric and magnetic fields from the potential vector by using usual expressions. We do not need in the present paper to reproduce explicitly the expressions of the third- and fifth-order modes (or Davis-Barton higher modes), on which our analysis will rely but see [180]. Let us nevertheless mention that electric and magnetic field expressions are found to be expanded as, e.g. Eqs. (4.16)–(4.21) in [4],

$$E_x = E_0\left[\psi_0 + s^2\left(\psi_2 + \frac{\partial^2\psi_0}{\partial\xi^2}\right) + \ldots\right]\exp(-ikz) \tag{10}$$

$$E_y = E_0\left[s^2\frac{\partial^2\psi_0}{\partial\xi\partial\eta} + s^4\frac{\partial^2\psi_2}{\partial\xi\partial\eta} + \ldots\right]\exp(-ikz) \tag{11}$$

$$E_z = E_0\left[-is\frac{\partial\psi_0}{\partial\xi} - is^3\left(\frac{\partial\psi_2}{\partial\xi} + i\frac{\partial^2\psi_0}{\partial\xi\partial\zeta}\right)\ldots\right]\exp(-ikz) \tag{12}$$

$$H_x = 0 \tag{13}$$

$$H_y = H_0\left[\psi_0 + s^2(\psi_2 + i\frac{\partial\psi_0}{\partial\zeta}) + \ldots\right]\exp(-ikz) \tag{14}$$

$$H_z = H_0\left[-is\frac{\partial\psi_0}{\partial\eta} - is^3\frac{\partial\psi_2}{\partial\eta} + \ldots\right]\exp(-ikz) \tag{15}$$

For further use, let us note, by comparing the expressions for the electric and magnetic fields, that the Davis-Barton scheme is not symmetric, a point to which we shall return later. Neglecting all terms with powers with respect to s greater than 1, and using Eqs. (8)-(9), we obtain explicitly what is the lowest order approximation in the Davis scheme, reading as:

$$E_y = H_x = 0 \tag{16}$$

$$E_x = E_0\psi_0\exp(-ikz) \tag{17}$$

$$E_z = -\frac{2Qx}{l}E_x \tag{18}$$

$$H_y = H_0\psi_0\exp(-ikz) \tag{19}$$

$$H_z = -\frac{2Qy}{l}H_y \tag{20}$$

These expressions define what has been called the order L of approximation, e.g. [4], p.100. Higher-order approximations are discussed in [180,181,187–189]. Conversely, we may use still simpler approximations. We indeed observe that longitudinal components are not zero in Eqs. (16)–(20), so that the fields do not describe a pure transverse wave, in contrast with the case of plane waves. Then, neglecting these components, we obtain a pure transverse wave, corresponding to what has been called the order L$^-$ of approximation, reading as, e.g. [4], pp.101-102:

$$E_y = H_x = E_z = H_z = 0 \tag{21}$$

$$\begin{pmatrix} E_x \\ H_y \end{pmatrix} = \begin{pmatrix} E_0 \\ H_0 \end{pmatrix}\psi_0\exp(-ikz) \tag{22}$$

This is actually the structure of the celebrated Kogelnik's model [190–192] as discussed in [4], pp.102–103. A still cruder approximation is the "tube-like" version in which the fields are transversely modulated by a Gaussian envelope of the form $\exp(-\rho^2/\rho_c^2)$ in which ρ is a cylindrical coordinate and ρ_c a characteristic transverse length related to the transverse "width" of the beam. Such a crude approximation may be sufficient in various situations, for instance to design an approximate theory of interaction between a Gaussian beam and a cylinder, e.g. [193], or to demonstrate that the laser light propagates slower than the speed of light, even in vacuum [194].

2.2. Divergence of the Davis scheme

The beam confinement factor s is a small parameter. It is exactly 0 for a plane wave ($w_0 \to \infty$). In the usual case of a commonly encountered Gaussian beam with a wavelength $\lambda = 0.5$ µm and $w_0 = 75$ µm, we have $s \approx 10^{-3}$. The largest value is obtained when the beam is strongly focused down to $w_0 \approx \lambda$, leading to $s \approx 1/(2\pi) \approx 1/6$. It has then been always believed that the series of Eq. (7) is convergent. We might then state that (i) none of the finite Davis-Barton modes is Maxwellian (they do not satisfy Maxwell's equations) but that (ii) Maxwell's equations are satisfied in the limit of the infinite Davis-Barton beam which (iii) generate an ideal finite solution to Maxwell's equations. This statement has been invalidated by Wang and Webb [179] who demonstrated that the Davis scheme of approximations is actually divergent. The demonstration of this fact is provided below departing however at a certain step from the original way used by Wang and Webb.

We begin by rewriting Eq. (6) using rescaled cylindrical coordinates ρ and ζ leading to:

$$\left(\frac{\partial^2}{\partial \rho^2}+\frac{\partial}{\rho \partial \rho}-2i\frac{\partial}{\partial \zeta}+s^2\frac{\partial^2}{\partial \zeta^2}\right)\psi=0 \tag{23}$$

in which we have used $\rho^2=\xi^2+\eta^2$. Rather than ρ and ζ, we now use two other independent variables q (which identifies with Q defined in Eq. (9)) and $\chi=\rho^2 q$, and we rewrite ψ as:

$$\psi=f(q,\chi)\exp(-i\chi)=f(q,\chi)\exp\left[\frac{-\rho^2(1+2i\zeta)}{1+4\zeta^2}\right] \tag{24}$$

After lengthy computations, Eq. (23) leads to:

$$\begin{aligned}&[i+s^2\chi q(\chi+2i)]f-[iq+2s^2q^2(1-i\chi)]f_q\\&-(1-i\chi)(1+2s^2\chi q)f_\chi-2s^2\chi q^2 f_{\chi q}-s^2q^3f_{qq}\\&-\chi(1+s^2\chi q)f_{\chi\chi}\\&=0\end{aligned} \tag{25}$$

in which the subscripts to f indicate derivatives in the usual way. We then look for a solution of the form:

$$\begin{bmatrix} a_{01}\neq 0 & a_{m>0,1} \\ \frac{a_{02}}{a_{01}} & a_{12} & \frac{a_{22}}{a_{02}} & a_{m>2,2} \\ \frac{a_{03}}{a_{01}} & a_{13} & \frac{a_{23}}{a_{03}} & \frac{a_{33}}{a_{03}} & \frac{a_{43}}{a_{03}} & a_{m>4,3} \\ \frac{a_{04}}{a_{01}} & a_{14} & \frac{a_{24}}{a_{04}} & \frac{a_{34}}{a_{04}} & \frac{a_{44}}{a_{04}} & \frac{a_{54}}{a_{04}} & \frac{a_{64}}{a_{04}} & a_{m>6,4} \\ \frac{a_{05}}{a_{01}} & a_{15} & \frac{a_{25}}{a_{05}} & \frac{a_{35}}{a_{05}} & \frac{a_{45}}{a_{05}} & \frac{a_{55}}{a_{05}} & \frac{a_{65}}{a_{05}} & \frac{a_{75}}{a_{05}} & \frac{a_{85}}{a_{05}} & a_{m>8,5} \\ \dots \end{bmatrix} \tag{35}$$

$$f(q,\chi)=\sum_{m,n=0}^{\infty}a_{mn}\chi^m q^n=\sum_{n=0}^{\infty}q^n\sum_{m=0}^{\infty}a_{mn}\chi^m=\sum_{n=0}^{\infty}q^n f_n(\chi) \tag{26}$$

in which we therefore introduced:

$$f_n(\chi)=\sum_{m=0}^{\infty}a_{mn}\chi^m \tag{27}$$

Inserting Eq. (26) into Eq. (25), we obtain a "recurrence-like" equation for the expansion coefficients a_{mn} reading as:

$$A_0+A_2s^2=0 \tag{28}$$

in which:

$$\begin{aligned}A_0=&[(m+1)(m+2)a_{m+2,n}-i(m+1)a_{m+1,n}]\chi^{m+1}q^n\\&+i(n+1)a_{m,n+1}\chi^m q^{n+1}\\&+[(m+1)a_{m+1,n}-ia_{mn}]\chi^m q^n\end{aligned} \tag{29}$$

$$\begin{aligned}A_2=&\left[(m+1)(m+2)a_{m+2,n}-2i(m+1)a_{m+1,n}-a_{mn}\right]\chi^{m+2}q^{n+1}\\&+\left[2(m+1)(n+1)a_{m+1,n+1}-2i(n+1)a_{m,n+1}\right]\chi^{m+1}q^{n+2}\\&+\left[2(m+1)a_{m+1,n}-2ia_{mn}\right]\chi^{m+1}q^{n+1}\\&+(n+1)(n+2)a_{m,n+2}\chi^m q^{n+3}\\&+2(n+1)a_{m,n+1}\chi^m q^{n+2}\end{aligned} \tag{30}$$

Let us isolate in Eqs. (29)-(30) the terms corresponding to χ^0q^0, χ^0q^1 and χ^1q^0 We respectively obtain:

$$a_{10}-ia_{00}=0 \tag{31}$$

$$a_{11}+ia_{01}-ia_{01}=0 \tag{32}$$

$$4a_{20}-2ia_{10}=0 \tag{33}$$

in which the sign $(-)$ was misprinted to $(+)$ in [179], while the other $\chi^m q^n$-terms imply:

$$\begin{aligned}&(m+1)^2a_{m+1,n}-i(m-n+1)a_{mn}\\&+s^2[(m+n-1)(m+n)a_{m,n-1}\\&-2i(m+n-1)a_{m-1,n-1}-a_{m-2,n-2}]\\&=0\end{aligned} \tag{34}$$

The recurrence rules are then found to be complete and coherent if we demand both $a_{1n}=0$ and $a_{mn}=0$ for $m>2n$. The condition $a_{1n}=0$ implies in particular that $a_{10}=0$ which, by virtue of Eq. (31), implies as well that $a_{00}=0$. Furthermore, from Eq. (32) we have $a_{11}=0$ as well which is in agreement with the first recurrence rule. The recurrence rules also imply both $a_{10}=0$ and $a_{20}=0$ so that Eq. (33) is satisfied. Departing from Wang and Webb's exposition, we may now arrange the expansion coefficients in a matrix having the following form $\mathbf{M}$ reading as:

with values given by:

$$\mathbf{M}=\begin{bmatrix} a_{01}\neq 0 & 0 \\ (is^2)2! & 0 & \frac{1}{2} & 0 \\ (is^2)^2 3! & 0 & \frac{1}{2} & \frac{i}{3} & \frac{1}{12} & 0 \\ (is^2)^3 4! & 0 & \frac{1}{2} & \frac{i}{3} & \frac{-1}{8} & \frac{i}{12} & \frac{1}{144} & 0 \\ (is^2)^4 5! & 0 & \frac{1}{2} & \frac{i}{3} & \frac{-1}{8} & \frac{-i}{30} & \frac{-37}{720} & \frac{i}{120} & \frac{1}{2880} & 0 \\ \dots \end{bmatrix} \tag{36}$$

Let us note that we may argue that $a_{00}=0$, in a way independent from the recurrence rules. Indeed the corresponding x-component A_{00} of the x-polarized potential vector $\mathbf{A}_{00}=(A_{00},0,0)$ may be written as, see Eqs. (3), (24), (26):

$$A_{00}=a_{00}\exp[-i(\chi+kz)]=a_{00}\exp(-ikz)\exp\left[\frac{-i(x^2+y^2)}{w_0^2(i+\frac{2z}{kw_0^2})}\right] \tag{37}$$

In the far-field, we then have:

$$\begin{aligned}A_{00}\to A_{00}^{ff}&=a_{00}\exp(-ikz)\exp\left[\frac{-ik(x^2+y^2)}{2z}\right]\approx a_{00}\exp(-ikz)\\&\approx a_{00}\exp(-ik\sqrt{x^2+y^2+z^2})=a_{00}\exp(-ikr)\end{aligned} \tag{38}$$

From $\mathbf{A}_{00}^{ff}=(A_{00}^{ff},0,0)$, we may evaluate a far-field electric field reading as, in the Lorenz gauge, e.g. Eq. (1.121) of [4]:

$$\mathbf{E}_{00}^{ff}=(E_{00}^{ff},0,0)=\frac{-ic}{kn_p}\,\text{grad}\,\text{div}\,\mathbf{A}_{00}^{ff}-i\omega\mathbf{A}_{00}^{ff} \tag{39}$$

From Eq. (38), we have $\mathrm{div}\,\mathbf{A}_{00}^{ff} \approx a_{00}\partial\exp(-ikz)/\partial x \approx 0$, so that E_{00}^{ff} exhibits the same behavior as A_{00}^{ff}, with $E_{00}^{ff} \approx -i\omega A_{00}^{ff} \approx -i\omega a_{00}\exp(-ikr)$. This would be an admissible behavior in the far-field if we had $a_{00} \sim 1/r$ in order to generate a spherical wave (therefore satisfying the law of conservation of energy). This would however conflicts with the fact that a_{00} must be a constant excepted if we set $a_{00} = 0$.

Returning to Eq. (36), of particular interest is its first column which may be obtained from Eq. (34) for $m = 0$. Indeed, for $m = 0$ and $n = 0$, we recover $a_{00} = 0$. For $m = 0$ and $n = 1$, we recover $a_{11} = 0$. But, for $m = 0$ and $n > 1$, we obtain:

$$a_{0n} = ins^2 a_{0,n-1} \tag{40}$$

that is to say:

$$a_{0n}/a_{01} = (is^2)^{n-1} n! \tag{41}$$

Let us now introduce, from Eq. (26):

$$g_n(q,\rho) = q^n \sum_{m=0}^{\infty} a_{mn}\rho^{2m} q^m \tag{42}$$

in which we recalled that $\chi = \rho^2 q$. We then readily obtain that $g_0(q,\rho) = a_{00} = 0$ and that $g_1(q,\rho) = qa_{01}$. This term corresponds to a lowest-approximation reading as, from Eqs. (24)–(26):

$$\psi_{lowest} = a_{01} q \exp(-iq\rho^2) \tag{43}$$

which, comparing with the corresponding lowest-order ψ_0 of Eq. (8), implies that $a_{01} = i$, and that $g_1(q,\rho) = iq$. Furthermore, substituting Eqs. (35)-(36) into Eq. (42), we have:

$$g_2(q,\rho) = iq\left[(is^2 q)^1 2!\left(1 + \frac{1}{2}\rho^4 q^2\right)\right] \tag{44}$$

$$g_3(q,\rho) = iq\left[(is^2 q)^2 3!\left(1 + \frac{1}{2}\rho^4 q^2 + \frac{i}{3}\rho^6 q^3 + \frac{1}{12}\rho^8 q^4\right)\right] \tag{45}$$

$$g_4(q,\rho) = iq\left[(is^2 q)^3 4!\left(1 + \frac{1}{2}\rho^4 q^2 + \frac{i}{3}\rho^6 q^3 - \frac{1}{8}\rho^8 q^4 + \frac{i}{12}\rho^{10} q^5 + \frac{1}{144}\rho^{12} q^6\right)\right] \tag{46}$$

$$g_5(q,\rho) = iq\left[(is^2 q)^4 5!\left(1 + \frac{1}{2}\rho^4 q^2 + \frac{i}{3}\rho^6 q^3 - \frac{1}{8}\rho^8 q^4 - \frac{i}{30}\rho^{10} q^5 - \frac{37}{720}\rho^{12} q^6 + \frac{i}{120}\rho^{14} q^7 + \frac{1}{2880}\rho^{16} q^8\right)\right] \tag{47}$$

These equations contain a leading primary term reading as:

$$P_n = (is^2 q)^{n-1} n! \tag{48}$$

satisfying the recurrence relation:

$$P_n = is^2 qnP_{n-1} \tag{49}$$

leading to:

$$\left|\frac{P_n}{P_{n-1}}\right| = s^2|q|n = \frac{ns^2}{\sqrt{1+4\zeta^2}} \tag{50}$$

In the large n limit, the ratio $|P_n/P_{n-1}|$ becomes larger than 1 indicating the divergence of the Davis scheme. This is confirmed by using Eq. (40) which leads to:

$$a_{0n} = (is^2)^{n-1} n! a_{01} \tag{51}$$

as confirmed by the first column of Eq. (36). The turning critical point is for $n_c = s^{-2}\sqrt{1+4\zeta^2}$ which, for $z = 0$, is simply $n_c = 1/s^2$.

For a plane wave ($s \to 0$), we have $n_c \to \infty$, independently of z. For $z = 0$, and a reasonable value of s equal to 10^{-3}, we have $n_c = 10^6$, while for the largest limit $s \sim 1/6$, we have $n_c \sim 40$, these values increasing when z increases. In any case, these values confirm the validity of the Davis approximations used in the literature, up to the seventh order beam. It is likely that other expansion approaches, similar to the Davis one, might be divergent as well although unnoticed. For instance, elaborating on the work by Agrawal and Pattanayak already quoted [184] and on an angular spectrum decomposition, Chen et al. [195], in 2002, expressed solutions to Maxwell's equations in terms of series with respect to powers of s (e.g. 7). Although they limited their analysis to first few terms of the expansion (as made explicitly in the Davis scheme), they however noticed a rapid divergence of higher-order terms which, although not explicitly demonstrated (as has been done above for the Davis scheme), certainly indicates that their scheme is certainly genuinely divergent in agreement with their statement (p 410) that, at some point, "the series expansion approach becomes invalid". It is worthwhile to note here that the angular spectrum decomposition has been of wide use in GLMT, e.g. a review in Section 3 of [196], and a recent paper devoted to the issue.

Our statement concerning Davis series is however stronger and more explicit because we claim that this expansion approach is *always* invalid beyond a certain critical $n_c \approx 1/s^2$. Another example, worth to be revisited, is by Seshadri, in 2008 [185] who used an expansion similar to the one of Eq. (7) to solve a Helmholtz equation, e.g. compare their Eq. (12) and (23) above.

3. The standard beam scheme and its divergence

The standard beam has been introduced in [187] as the consequence of a comprehensive investigation of the Davis scheme of approximations, aiming to a justification of a localized approximation (which will be discussed in Sections 4 and 5). It is expressed in terms of BSCs in the framework of GLMT. We therefore begin by recalling a small but necessary background concerning GLMT.

3.1. GLMT-background

In this subsection, we follow the convention and notations of [187] which expressed the GLMT in terms of electric field **E** and magnetic field **B**, instead of the more usual electric field **E** and magnetic field **H** (**B** =μ**H**). The incident field is then encoded by two sets of BSCs denoted as $g_{n,TM}^m$ and $g_{n,TE}^m$ with TM standing for "Transverse magnetic", TE for "Transverse electric", with n ranging from 1 to ∞, and m ranging from $(-n)$ to $(+n)$. These BSCs may be evaluated by double quadratures or triple quadratures [197,198] in which $g_{n,TM}^m$ and $g_{n,TE}^m$ depend on the radial components of the electric E_r and magnetic B_r fields respectively. The double quadrature formulation may be written as [187]:

$$g_{n,TM}^m = \frac{-(i^{n-1})}{4\pi}\frac{R}{j_n(R)}\frac{(n-|m|)!}{(n+|m|)!} \times \int_0^{\pi}\sin\theta d\theta\int_0^{2\pi} d\phi P_n^{|m|}(\cos\theta) \exp(-im\phi)\frac{E_r(R,\theta,\phi)}{E_0} \tag{52}$$

$$g_{n,TE}^m = \frac{-(i^{n-1})}{4\pi}\frac{R}{j_n(R)}\frac{(n-|m|)!}{(n+|m|)!} \times \int_0^{\pi}\sin\theta d\theta\int_0^{2\pi} d\phi P_n^{|m|}(\cos\theta) \exp(-im\phi)\frac{cB_r(R,\theta,\phi)}{n_p E_0} \tag{53}$$

in which $R = kr$, (r,θ,ϕ) are spherical coordinates, $P_n^{|m|}(\cos\theta)$ are associated Legendre functions in the Hobson's notation [199], $j_n(R)$

are spherical Bessel functions of the first kind, E_0 is the electric field strength and n_p is the refractive index. If the electric and magnetic fields exactly satisfy Maxwell's equations, the R-dependent prefactors will eventually disappear – as we shall observe – because the integrals θ and ϕ are proportional to $j_n(R)/R$ (this is compulsory because the coherence of the GLMT framework implies that the BSCs are constant complex numbers which do not depend on the coordinates).

Of special interest in this paper is now to consider an incident Gaussian beam in the configuration of Fig. 1 which is called an on-axis configuration. In such a configuration, the radial components of the incident fields reduce to:

$$E_r(R,\theta,\phi) = E_0 \exp(-iR\cos\theta) F_e(R,\theta) \sin\theta \cos\phi \tag{54}$$

$$B_r(R,\theta,\phi) = B_0 \exp(-iR\cos\theta) F_b(R,\theta) \sin\theta \sin\phi \tag{55}$$

with $B_0 = n_p E_0/c$. The quadratures in Eqs. (52) and (53) may then be performed analytically. It is then found that only the $(m = \pm 1)$ BSCs are non-zero and that these non-zero BSCs allow one to introduce reduced uni-index BSCs g_n according to:

$$g^m_{n,TM} = \frac{1}{2} g_{n,e} \delta_{m,\pm 1} \tag{56}$$

$$g^m_{n,TE} = \mp \frac{i}{2} g_{n,b} \delta_{m,\pm 1} \tag{57}$$

in which:

$$g_{n,e} = \frac{-i^{n-1}}{2} \frac{R}{j_n(R)} \frac{1}{n(n+1)} \int_0^\pi \sin^2\theta F_e(R,\theta) \exp(-iR\cos\theta) P^1_n(\cos\theta) d\theta \tag{58}$$

$$g_{n,b} = \frac{-i^{n-1}}{2} \frac{R}{j_n(R)} \frac{1}{n(n+1)} \int_0^\pi \sin^2\theta F_b(R,\theta) \exp(-iR\cos\theta) P^1_n(\cos\theta) d\theta \tag{59}$$

3.2. Return to Davis scheme

The solution to Eq. (6), limited to a few first terms (before reaching the diverging critical turning point), may be written as a series in powers of s^2 according to Davis [162], Barton and Alexander [180], Lock and Gouesbet [187]:

$$\psi = D_0 \exp(-\rho^2 D_0)[1 + s^2(2D_0 - \rho^4 D_0^3) + s^4(6D_0^2 - 3\rho^4 D_0^4 - 2\rho^6 D_0^5 + \frac{1}{2}\rho^8 D_0^6) + O(s^6)] \tag{60}$$

in which:

$$D_0 = \frac{1}{1 - 2i\zeta} = iQ \tag{61}$$

The Davis first-order, third-order and fifth order Davis beams are obtained from Eq. (60) by only retaining some truncations in the equation, namely up to $O(s^0)$, $O(s^2)$ and $O(s^4)$ respectively. Using respectively the superscripts $D1, D3$ and $D5$ to identify the various beams, we then have:

$$\psi^{D1} = D_0 \exp(-\rho^2 D_0) \tag{62}$$

$$\psi^{D3} = D_0 \exp(-\rho^2 D_0)[1 + s^2(2D_0 - \rho^4 D_0^3)] \tag{63}$$

$$\psi^{D5} = D_0 \exp\left(-\rho^2 D_0\right)[1 + s^2(2D_0 - \rho^4 D_0^3) + s^4(6D_0^2 - 3\rho^4 D_0^4 - 2\rho^6 D_0^5 + \frac{1}{2}\rho^8 D_0^6)] \tag{64}$$

Eqs. (62)–(64) then provide three successive approximations of the potential vector of Eq. (3), from which we may deduce three successive approximations of the electric $\mathbf{E}$ and magnetic $\mathbf{B}$ fields, and therefore three successive approximations of the radial components E_r and B_r which allow one to evaluate the BSCs $g_{n,e}$ and $g_{n,b}$ from Eqs. (58)-(59). The electric and magnetic fields obtained however contain additional dependences with respect to s. We may then develop different approaches depending on the way to deal with the s -dependent additional terms. These approaches are called (i) the mathematical conservative version which corresponds to truncations of the fields at $O(s^1)$, $O(s^3)$ and $O(s^5)$ for the successive approximations, (ii) the L -version in the sense given to this terminology in [1,4,200–202], e.g. Eqs. (16)–(20) for the first-order beam and (iii) the symmetrized Davis-Barton version.

Indeed, we already observed from Eqs. (10)–(15) that the Davis scheme lacks of symmetry. Although this lack of symmetry does not occur in Eqs. (16)–(20) of the first order beam, it would occur for higher-order beams. The origin of this lack of symmetry is simple. Indeed, we started from a potential vector which was polarized in the x-direction. The relation $\mathbf{B} = \nabla \times \mathbf{A}$ then implies that the x-component of $\mathbf{B}$ vanishes, as we can see from Eq. (13), in contrast with Eq. (10). The symmetry is restored when we add a potential vector which is formally identical to the previous x-polarized one, but which is polarized in the y-direction, leading to the symmetrized Davis-Barton version. After a considerable amount of computations, we then find that:

$$F_e(R,\theta) = D_0 \exp(-s^2 R^2 D_0 \sin^2\theta) h_e(R,\theta) \tag{65}$$

$$F_b(R,\theta) = D_0 \exp(-s^2 R^2 D_0 \sin^2\theta) h_b(R,\theta) \tag{66}$$

with:

$$h^{DB1} = h_e^{DB1} = h_b^{DB1} = D_0 \tag{67}$$

$$h^{DB3} = h_e^{DB3} = h_b^{DB3} = D_0(1 + 3s^4 D_0^2 R^2 \sin^2\theta - s^6 D_0^3 R^4 \sin^4\theta) \tag{68}$$

$$h^{DB5} = h_e^{DB5} = h_b^{DB5} = D_0(1 + 3s^4 D_0^2 R^2 \sin^2\theta - s^6 D_0^3 R^4 \sin^4\theta + 10 s^8 D_0^4 R^4 \sin^4\theta - 5 s^{10} D_0^5 R^6 \sin^6\theta + \frac{1}{2} s^{12} D_0^6 R^8 \sin^8\theta) \tag{69}$$

for the first-order, third-order and fifth-order respectively, with the immediate consequences that the double set of BSCs $g_{n,e}$ and $g_{n,b}$ reduces to a single set of coefficients $g_n = g_{n,e} = g_{n,b}$.

3.3. Beam shape coefficients

Inserting Eqs. (67)–(69) into Eqs. (65)-66, thereafter into either Eqs. (58) or (59), we obtain integrals which, after a bit of effort, can be integrated analytically, leading to:

$$g_n^{DB1} = 1 - s^2(n-1)(n+2) + NCT^{DB1} \tag{70}$$

$$@ccc@g_n^{DB3} = g_n^{DB1} + \frac{1}{2}s^4(n-2)(n-1)(n+2)(n+3) - \frac{1}{6}s^6(n-3)(n-2)(n-1)(n+2)(n+3) + NCT^{DB3} \tag{71}$$

$$g_n^{DB5} = g_n^{DB3} + \frac{1}{24}s^8(n-4)(n-3)(n-2)(n-1)(n+2)(n+3)(n+5) - \frac{1}{120}s^{10}(n-5)(n-4)(n-3)(n-2)(n-1) \times (n+2)(n+3)(n+5)(n+6) + NCT^{DB5} \tag{72}$$

These expressions exhibit (i) terms which depend only on n and s, but which do not depend on any coordinate and (ii) non-constant terms (abbreviated as NCT) which depend on n and s, but depend as well on the coordinate R. These NCTs are $O(s^4)$, $O(s^8)$ and $O(s^{12})$ for $DB1$, $DB3$ and $DB5$ respectively. They are the consequence of the fact that none of the Davis beams of limited order is Maxwellian. It is worthwhile to insist on the beauty of these results, particularly when the amount of computations required to reach them is taken into account. They emphasize indeed a beautiful amount of unexpected symmetries which leads the researcher to the idea that something deep has indeed been reached by the procedure, and that we may rely on it for further investigations.

In [187], these results have been summarized under the form:

$$g_n^{DBk} = \sum_{p=0}^{k} \frac{(-1)^p s^{2p}}{p!} \frac{(n-1)!}{(n-1-p)!} \frac{(n+1+p)!}{(n+1)!} + NCT^{DBk} \tag{73}$$

which is valid for $k = 1, 3$ and 5. This expression, although "correct", may be found dangerous as far as $(n-1-p)!$ may apparently have no meaning. For instance, for $n = 1$, it leads to $(-1)!...(-5)!$ for $l = 1 \ldots 5$. In the present paper, we shall prefer to write a somewhat more explicit expression reading as:

$$g_n^{DBk} = \sum_{p=0}^{k} \frac{(-1)^p s^{2p}}{p!} N_{np} + NCT^{DBk} \tag{74}$$

in which:

$$N_{n0} = 1 \tag{75}$$

$$N_{np} = (n-p)(n-p+1)\ldots(n-2)(n-1) \\ (n+2)(n+3)\ldots(n+p+1),\ p > 0 \tag{76}$$

Although not used in the previous literature, it is worthwhile to note that the symbol N_{np} may be expressed, in two ways, in terms of the Pochhammer's symbol reading as:

$$(\alpha)_0 = 1 \tag{77}$$

$$(\alpha)_k = \alpha(\alpha+1)\ldots(\alpha+k-1) \tag{78}$$

so that Eq. (74) may be rewritten in two ways as:

$$\begin{aligned} g_n^{DBk} &= \sum_{p=0}^{k} \frac{(-1)^p s^{2p}}{p!} (n-p)_p (n+2)_p + NCT^{DBk} \\ &= \sum_{p=0}^{k} \frac{(-1)^p s^{2p}}{p!} \frac{(n-p)_{2(p+1)}}{n(n+1)} + NCT^{DBk} \end{aligned} \tag{79}$$

In the sequel, we shall go on using the more concise symbol N_{np}, but when it is useful to proceed otherwise. These computations may be generalized to the case when $z_0 \neq 0$. One then obtains, after much algebra [187]:

$$g_n^{DBk} = \exp(ikz_0) \sum_{j=0}^{j+2p=2k+1} \sum_{p=0} \left(-2is\frac{z_0}{w_0}\right)^j \frac{(-1)^p s^{2p}}{p!} \frac{(p+j)!}{j!p!} N_{np} + NCT^{DBk} \tag{80}$$

3.4. Standard beams: Divergence for the case $z_0 \neq 0$

Standard beams are then introduced as the infinite generalization of Eqs. (74) and (80), reading as [182,187]:

$$g_n = \sum_{p=0}^{\infty} \frac{(-1)^p s^{2p}}{p!} N_{np} \tag{81}$$

$$g_n = \exp(ikz_0) \sum_{j=0}^{\infty} \sum_{p=0}^{\infty} \left(-2is\frac{z_0}{w_0}\right)^j \frac{(-1)^p s^{2p}}{p!} \frac{(p+j)!}{j!p!} N_{np} \tag{82}$$

for $z_0 = 0$ and $z_0 \neq 0$ respectively, the last one being as well available as:

$$g_n = \exp(ikz_0) \sum_{j=0}^{\infty} \sum_{p=0}^{\infty} \left(-2is\frac{z_0}{w_0}\right)^j \frac{(-1)^p s^{2p}}{p!} \frac{(p+j)!}{j!p!} \frac{(n-1)!(n+1+p)!}{(n-1-p)!(n+1)!} \tag{83}$$

which define beams which are exactly Maxwellian (i.e. which exactly satisfy Maxwell's equations) and are proposed as providing an exact definition of Gaussian beams, hence the name of standard beams. It was conjectured that such beams would be the limit of a complete Davis procedure if it were achieved. We now know that the Davis procedure is divergent, as demonstrated in Section 2, but leaves open the question to know whether the standard beam procedure is divergent as well.

A first step to the answer is to remember that, when dealing with the applications of standard beams to the evaluation of radiation pressure forces, it has been observed that Eq. (82) possesses a finite radius of convergence [203]. To understand this feature, it will be sufficient to discuss the issue for $n = 1$. We then have (for $n = 1$, it is more expedient to use Eq. (83) and the fact that factorials of negative integers are not defined):

$$g_1 = \exp(ikz_0) \sum_{j=0}^{\infty} (-2is\frac{z_0}{w_0})^j \tag{84}$$

For further use, note that N_{np} does not appear any more for this case. We then introduce the change of variables $\mathcal{A} = 2sz_0/w_0 = 2z_0/l$, and use the four-valued periodicity of i^m $(m = 0, 1\ldots)$ to rewrite Eq. (84) as a summation of four partial series reading as:

$$g_1 = \sum_{i=1}^{4} S_i \tag{85}$$

in which S_i is the limit when $q \to \infty$ of S_i^q reading as:

$$\begin{aligned} \begin{pmatrix} S_1^q \\ S_2^q \\ S_3^q \\ S_4^q \end{pmatrix} &= \begin{pmatrix} 1 \\ -i\mathcal{A} \\ -\mathcal{A}^2 \\ i\mathcal{A}^3 \end{pmatrix} \exp(ikz_0)(1 + \mathcal{A}^4 + \mathcal{A}^8 + \ldots + \mathcal{A}^{4q}) \\ &= \begin{pmatrix} 1 \\ -i\mathcal{A} \\ -\mathcal{A}^2 \\ i\mathcal{A}^3 \end{pmatrix} \exp(ikz_0) \frac{1 - \mathcal{A}^{4(q+1)}}{1 - \mathcal{A}^4} \end{aligned} \tag{86}$$

leading to:

$$g_1 = \lim_{q\to\infty} \exp(ikz_0) \frac{1 - \mathcal{A}^{4(q+1)}}{1 - \mathcal{A}^4} (1 - i\mathcal{A} - \mathcal{A}^2 + i\mathcal{A}^3) \tag{87}$$

which may be rewritten as:

$$g_1 = \lim_{q\to\infty} \exp(ikz_0) \frac{1 - \mathcal{A}^{4(q+1)}}{1 + i\mathcal{A}} \tag{88}$$

The convergence of g_1 then depends on the value of $\mathcal{A}$ according to the following rules:

(i) When $|\mathcal{A}|$ is smaller than 1, i.e. $|z_0| < l/2$, then the term $\mathcal{A}^{4(q+1)}$ in Eq. (88) tends to 0 and g_1 is well defined.

(ii) Otherwise, i.e. $|\mathcal{A}| > 1$, then g_1 diverges.

Therefore, the standard expression for g_1 exhibits a finite radius of convergence. This can easily be generalized to g_n by retaining only the term $p = 0$ in Eq. (83). This feature explains why computations of optical forces were only possible in a small neighborhood of the beam waist center in [106]. Hence, the standard scheme had to be improved as described in the next section.

4. Improved standard beams and localized beam models

4.1. Improved standard beams

Since we have to deal with the case $z_0 \neq 0$, detailed computations would be heavy to report and we shall therefore be content with a sketch of the procedure. Let us consider Eqs. (65)-(66), which imply that, for the symmetrized Davis-Barton version, we may write (with obvious superscripts):

$$F^k(R,\theta) = F_e^k(R,\theta) = F_b^k(R,\theta) = D_0 \exp(-s^2R^2D_0 \sin^2\theta)h^{DBk}(R,\theta) \tag{89}$$

which is valid for $z_0 = 0$. For $z_0 \neq 0$, D_0 must be replaced by D reading as [187]:

$$D = \frac{1}{1 - 2i\zeta + i\mathcal{A}} \tag{90}$$

so that we now have:

$$F^k(R,\theta) = D\exp(-s^2R^2D\sin^2\theta)h^{DBk}(R,\theta) \tag{91}$$

in which the h^{DBk}'s have to be generalized as well to the case $z_0 \neq 0$. In contrast with the procedure for the standard beams in which $F^k(R,\theta)$ was Taylor expanded with respect to s, we now expand them with respect to $\cos\theta$, which leads to the occurrence of an exponential term reading as:

$$\exp(\frac{-s^2R^2}{1+i\mathcal{A}}) \tag{92}$$

which is itself Taylor expanded but now with respect to R^2. Integrals required to obtain the BSCs are again analytically evaluated as we have done for $z_0 = 0$, non constant terms are again removed, and the expressions obtained for the first-, third- and fifth-order symmetrized Davis-Barton beams are generalized to obtain [203]:

$$g_n = \frac{\exp(ikz_0)}{1+i\mathcal{A}} \sum_{p=0}^{\infty} \frac{1}{(1+i\mathcal{A})^p} \frac{(-1)^p s^{2p}}{p!} N_{np} \tag{93}$$

which is to be compared with Eq. (83). We see that the summation over j which was at the origin of the divergence of the standard beam scheme has been cancelled out. The convergence of the improved standard beam scheme (when calculating the BSCs) is ensured by the fact that the terms N_{np} of Eq. (93) all vanish as soon as $n = p$ (see Eq. (76)) so that the series of Eq. (93) is actually a finite series when n is finite. This is in practice always the case since computations are made with numerical truncations. This does not imply however (i) that the converged values of the BSCs have converged to a correct value nor that (ii) the series used to evaluate the fields are indeed convergent. These questions will be answered in Section 5.

4.2. Localized approximations and localized beam models

When numerically integrating Eqs. (52)-(53) for Gaussian beams, the computational costs and times were prohibitive, except for very small particles, this being particularly true if we remember that such computations have been carried out in the eighties. Two approaches have been found to solve the problem (i) the development of finite series [204,205] and (ii) the development of so-called localized approximations which may be viewed as well, in the case of Gaussian beams, as the development of localized beam models. These localized beam models indeed generate Maxwellian Gaussian beams although they are built on paraxial non-Maxwellian Gaussian beams. We say that localized approximations (beam models) for Gaussian beams amount to a remodeling of the original descriptions, from non-Maxwellian descriptions to Maxwellian descriptions. These models have originally been developed in a somewhat heuristic way, relying on the van de Hulst localization principle [206,207] without any firm mathematical basis, and justified in an empirical way, e.g. [201,208]. This technique is reviewed in [209], to be completed with [210,211], and by warnings concerning the use of localized approximations for beams exhibiting axicon angles, e.g. [212,213] and/or topological charges, e.g. [214,215]. The localized procedure may be summarized as follows [216].

(i) Expand the radial component of the electric field in terms of m -waves, proportional to $\exp(im\phi)$, according to:

$$E_r = \sum_{m=-\infty}^{m=+\infty} E_r^m \tag{94}$$

(ii) Extract the non-plane-wave contribution $\mathcal{E}_r^m(R = kr, \theta)$ of E_r^m.

(iii) Then, the localized approximation $\overline{g_{n,TM}^m}$ of the BSC $g_{n,TM}^m$ reads as:

$$\overline{g_{n,TM}^m} = (\frac{-i}{L^{1/2}})^{|m|-1}\mathcal{E}_r^m(L^{1/2}, \pi/2) \tag{95}$$

In the original localized approximation, $R = L^{1/2}$, called the radial evaluation point, was taken to be equal to $R = (n + 1/2)$ [205,217,218]. The justification of the procedure in the case of Gaussian beams has been developed in [187] for on-axis beams and in [188] for off-axis beams. In the case of on-axis beams to which we currently restrict our analysis, the radial evaluation point R is modified to $\sqrt{(n-1)(n+2)}$ and the localized approximation is found to read as [187]:

$$g_n^{loc} = \frac{\exp(ikz_0)}{1+i\mathcal{A}} \exp\left[\frac{-s^2(n-1)(n+2)}{1+iA}\right] \tag{96}$$

which, for $z_0 = 0$, leads to:

$$g_n^{loc} = \exp[-s^2(n-1)(n+2)] = 1 - s^2(n-1)(n+2) + \ldots \tag{97}$$

to be compared with Eq. (70). For a general demonstration adapted to the case of off-axis "arbitrary shaped beams", see [216].

5. Numerical illustrations

To complete numerical results and discussions available from Gouesbet et al. [182], Lock and Gouesbet [187], Gouesbet and Lock [188], Polaert et al. [203], Ren et al. [219], we now provide extra-results concerning the schemes discussed above, namely localized approximations and improved standard beams, being content to discuss the on-axis case for $z_0 = 0$, either using Eq. (97) for the improved localized approximation or Eq. (81) of the original standard beam which identifies with Eq. (93) of the improved standard beam when $z_0 = 0$. We shall then display $I = |E_x/E_0|^2$ in the xy plane (i.e. for $\theta = \pi/2$) along the x-axis (i.e. for $\phi = 0$), according to:

$$I = |E_x/E_0|^2 = |E_r(\theta = \pi/2, \phi = 0)/E_0|^2 \tag{98}$$

in which E_r reads as, e.g. Eqs. (3.3) and (3.39)–(3.45) in [4]:

$$E_r = E_0 \sum_{n=1}^{\infty} \sum_{m=-n}^{+n} (-i)^{n+1} \frac{2n+1}{n(n+1)} g_{n,TM}^m [\psi_n''(kr) + \psi_n(kr)] P_n^{|m|}(\cos\theta) \exp(im\phi) \tag{99}$$

in which $\psi_n(kr)$ denotes Ricatti-Bessel functions of the first kind. In the present case in which Eq. (56) is valid with $g_{n,e} = g_n$, Eq. (99) leads to:

$$E_r(r, \theta = \pi/2, \phi = 0) = \frac{E_0}{kr} \sum_{n=1}^{\infty} (-i)^{n+1}(2n+1) g_n j_n(kr) P_n^1(0) \tag{100}$$

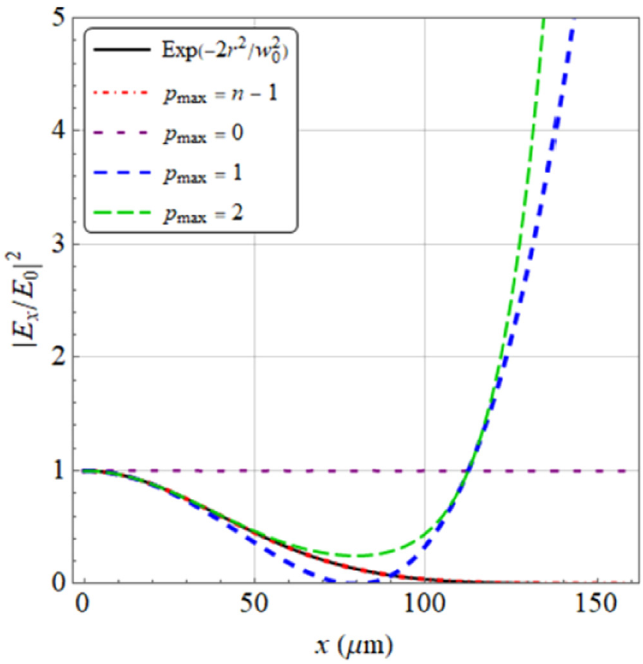

Fig. 2. Standard beams, $s = 10^{-3}$.

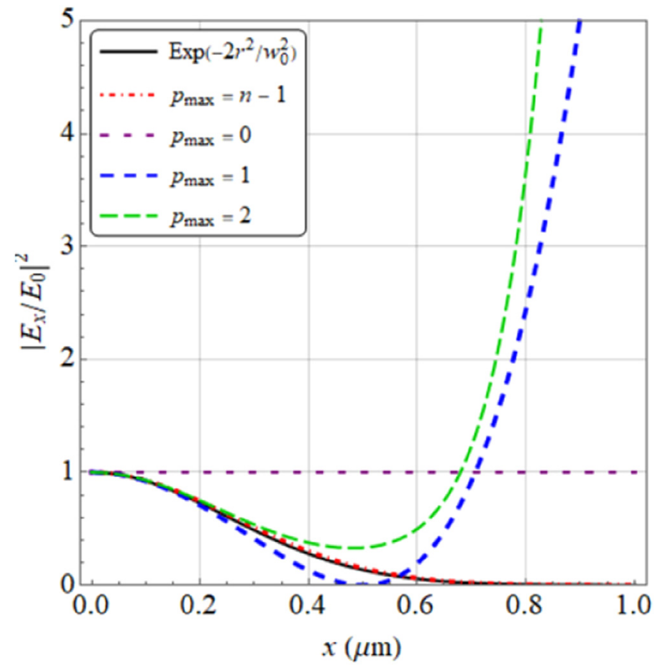

Fig. 4. Standard beams, $s = 1/(2\pi)$.

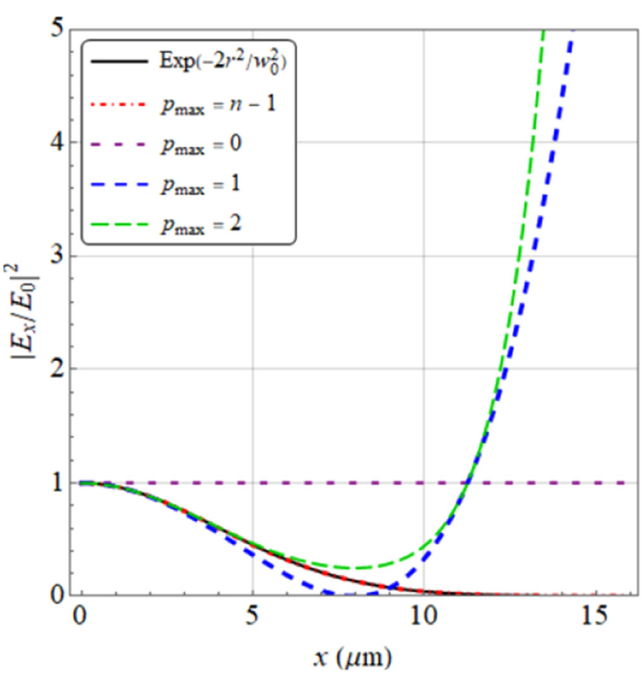

Fig. 3. Standard beams, $s = 10^{-2}$.

in which we have used:

$$\psi_n''(kr) + \psi_n(kr) = \frac{n(n+1)}{kr} j_n(kr) \tag{101}$$

Calculations have been carried out using the commercial software *Wolfram 12.1 Student Edition*, and were run on a personal laptop [Intel(R) Core(TM) 17-3630QM CPU @ 2.40GHz, 16.0 GB]. The figures are displayed for $\lambda = 0.5$ μm and three values of s, namely $s = 10^{-3}$ (corresponding to a loosely focused beam with $w_0 \approx 80$ μm), $s = 10^{-2}$ (corresponding to a more focused beam with $w_0 \approx 8$ μm), and $s = (1/2\pi)$ (corresponding to a very focused beam in the limit $w_0 = \lambda$).

Fig. 2 exhibits the intensity I versus x expressed in μm using the standard (or improved) standard beam expression of Eq. (81), in which the summation is carried from 0 to p_{max}, with four values of p_{max} from 0 to $(n-1)$. For $p_{max} = 0$, the BSCs g_n are all equal to 1 and the intensity is found to be a constant. For $p_{max} = 1$ and 2, the intensity begins to decrease like approaching a Gaussian shape before blowing up. The maximal value of p_{max} is $(n-1)$ since the BSCs become all 0 as soon as p reaches the value n. For this value the intensity exhibits a Gaussian profile which cannot be distinguished on the figure from the one given by $\exp(-2r^2/w_0^2)$. Figures 3 and 4 correspond to $s = 10^{-2}$ and $s = 1/(2\pi)$ respectively, with similar comments. Note however (i) that the increase of s corresponds to a stronger focusing and therefore to a decrease of the lateral extension of the beam, from 150 for $s = 10^{-3}$ to 1.0 for $s = 1/(2\pi)$ and (ii) that, even for the strongest focusing, the intensity profile is still very close to an ideal Gaussian profile. Remember, however, that the identification between the intensity profile reconstructed using the BSCs and the one ideally defined by $\exp(-2r^2/w_0^2)$ needs not to be perfect since the former, built with BSCs, perfectly satisfies Maxwell's equations, in contrast with the tube-like beam defined by an ideal profile.

In Fig. 5, we compare the intensities provided either by using the improved standard scheme of Eq. (93) specified for $z_0 = 0$, i.e. Eq. (81), or the localized approximation of Eq. (97), for $s = 10^{-3}$, showing very good agreement between the two approaches. The ideal Gaussian profile is displayed as well, showing that the Gaussian profile (corresponding to a non-Mawellian beam) agrees well with the reconstructed profiles, based on BSCs g_n (corresponding to Maxwellian beams). Fig. 6. is the same as Fig. 5, but for $s = 10^{-2}$, and would be commented in exactly the same way. Similarly, Fig. 7. is for $s = 1/(2\pi)$. The three profiles are slightly different, with the improved standard scheme being slightly better than the profile corresponding to the localized approximation. The price for this tiny improvement is however heavy: (i) the improved standard scheme requires the use of infinite precision computations and (ii) it is much more demanding in terms of computational times. Indeed, the calculations with the localized approximation are in practice "instantaneous", in contrast with the use of the standard scheme which demanded about 2 s for $s = 1/(2\pi)$,

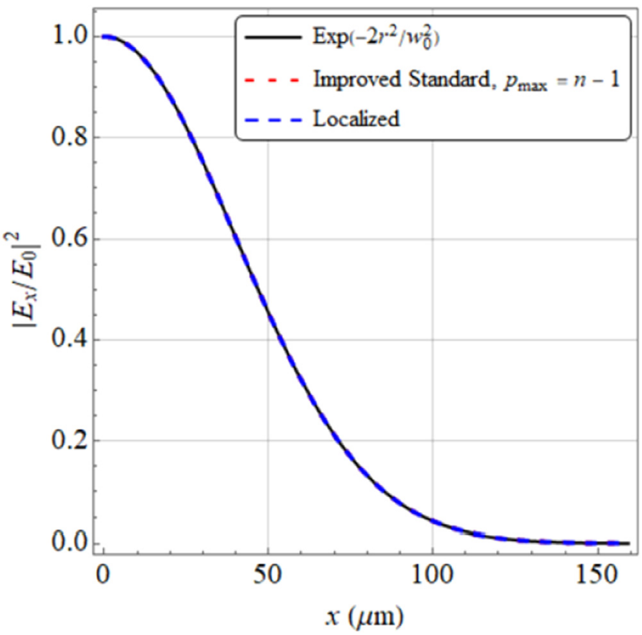

Fig. 5. Comparison between intensities, $s = 10^{-3}$.

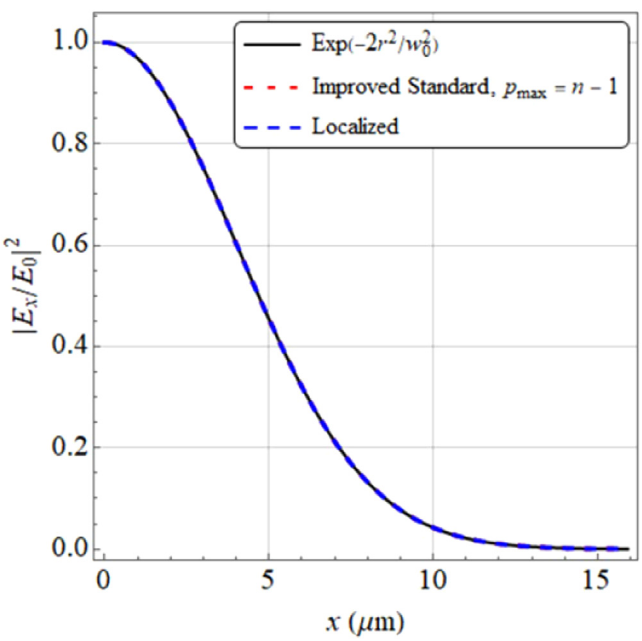

Fig. 6. Comparisons between intensities, $s = 10^{-2}$.

about 129 s for $s = 10^{-2}$ and more than 14 h for $s = 10^{-3}$. Besides, we have to face to another impediment, namely that the improved standard scheme is certainly divergent as we are going to discuss in the next subsection.

5.1. Divergence of the improved standard scheme

Although the improved standard scheme allows one to evaluate BSCs without any divergence (since they are evaluated using finite series), it unfortunately happens that, as a whole, it looks to be divergent as we shall discuss in this subsection, so that the conjecture according to which it would provide a perfectly accurate scheme is actually not satisfied (an unexpected result indeed). To this purpose, let us consider Eq. (81) which, by using the Pochhammer's symbol of Eqs. (77), (78), may be rewritten as, using a gen-

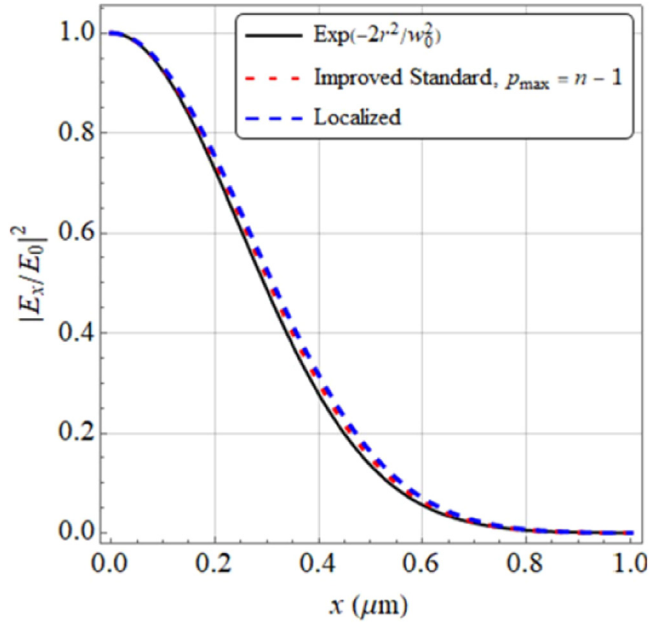

Fig. 7. Comparisons between intensities, $s = 1/2\pi$.

eralization of Eq. (79):

$$g_n = \frac{1}{n(n+1)}\sum_{p=0}^{n-1}\frac{(-1)^p s^{2p}}{p!}(n-p)_{2(p+1)} = \frac{1}{n(n+1)}\sum_{p=0}^{n-1}(-1)^p X_p \tag{102}$$

which provides a definition of X_p. Furthermore, we have explicitly taken into account the fact N_{np} is 0 for $p \geq n$, to insist on the fact that, being evaluated by finite series, the values of the BSCs of the improved standard scheme do indeed converge. It is however readily shown that:

$$\frac{X_p}{X_{p-1}} = s^2(n-p)\frac{n+p+1}{p} > s^2(n-p) \tag{103}$$

Eq. (103) implies that X_p becomes greater than X_{p-1} when $s^2(n-p)$ becomes greater than 1. In a summation from $p = 0$ to $p = n-1$, the most dangerous value is for $p = 0$ which defines a critical value of n given by $n_c s^2 \approx 1$, i.e. $n_c \approx 1/s^2$. Let us note that this critical value is the same as the one we evaluated for the divergence of the Davis scheme, e.g. comment after Eq. (51). Considering Eq. (100) in which BSCs are required for $n = 1$ to ∞, there is then the risk that $E_r(r, \theta = \pi/2, \phi = 0)$ might diverge so that, eventually, the improved standard scheme would become a divergent scheme under conditions similar to the ones of the Davis scheme, and that correct results as obtained in the previous subsection would require a well chosen truncation of the series such as the one of Eq. (100).

We now illustrate these results with complementary numerical data obtained for a tighly focused beam with $s = 1/(2\pi)$, therefore limiting the critical value of n_c to about 40 in order to limit the computational time. Fig. 8 displays the value of the BSCs g_n versus n. After decreasing down to 0, we then indeed observe a blowing-up for about the expected critical value of n. Remember however, once again, that these BSCs are evaluated using finite series so that convergence is ensured, but the observed blowing-up may have disastrous consequences when evaluating field components. To illustrate this issue, let us consider $E_r(r, \theta = \pi/2, \phi = 0)$ of Eq. (100), from which we extract:

$$E_n = \left|\frac{1}{kr}(-i)^{n+1}(2n+1)g_n j_n(kr)P_n^1(0)\right| \tag{104}$$

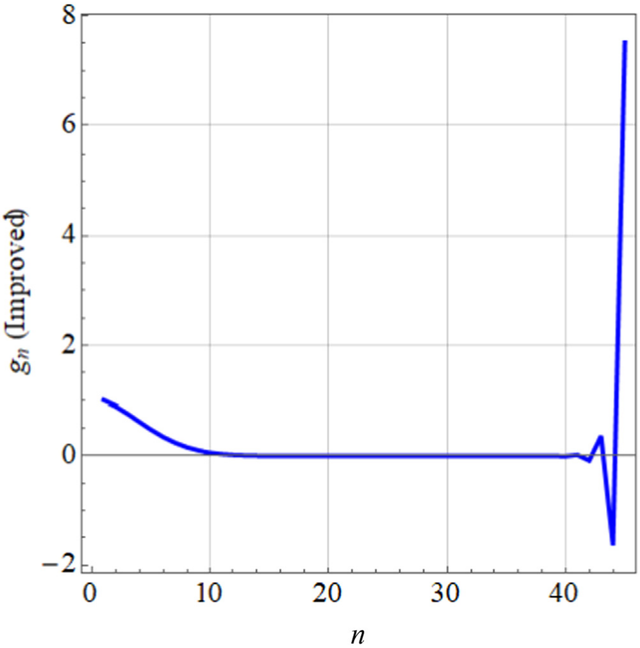

Fig. 8. BSCs versus n. Improved standard scheme.

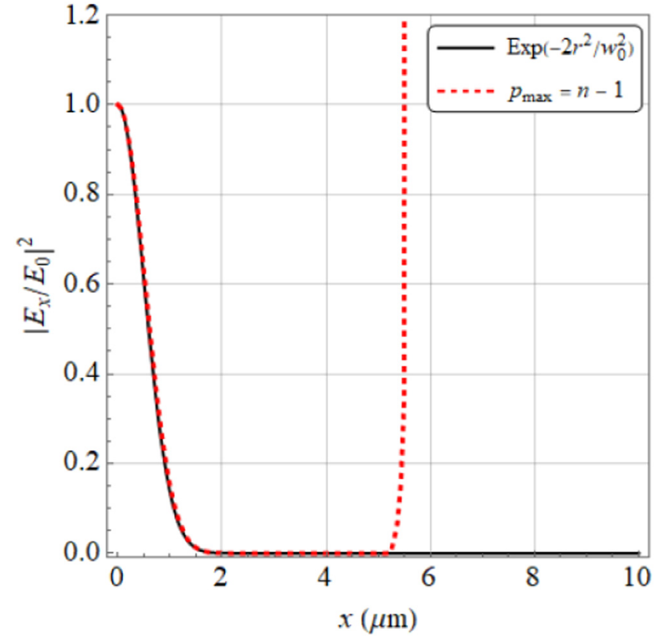

Fig. 10. Intensity versus x, $s = 1/(2\pi)$.

Fig. 9. then displays E_n versus x/w_0 for various values of n. The blowing-up of E_n is well apparent if we look at the values of the vertical scales, starting from about 1. for $n = 1$, decreasing to about 10^{-11} for $n = 35$ and, after the critical value $n = 40$, increasing to 10^{-3} for $n = 41$, and reaching about 10^{44} for $n = 75$. The consequence of such a blowing-up is illustrated in Fig. 10. which displays the intensity I versus x. We may distinguish (i) a first region from $x = 0$ to $x = 4$ where the intensity correctly agrees with the ideal Gaussian profile followed by a second blowing-up region, indicating a divergence of the scheme. This fact does not prevent to obtain correct results, with the condition that the results obtained have to be rejected after a certain critical value of x. As for the Davis scheme, this is a typical behaviour of asymptotic series that we shall discuss in the next section.

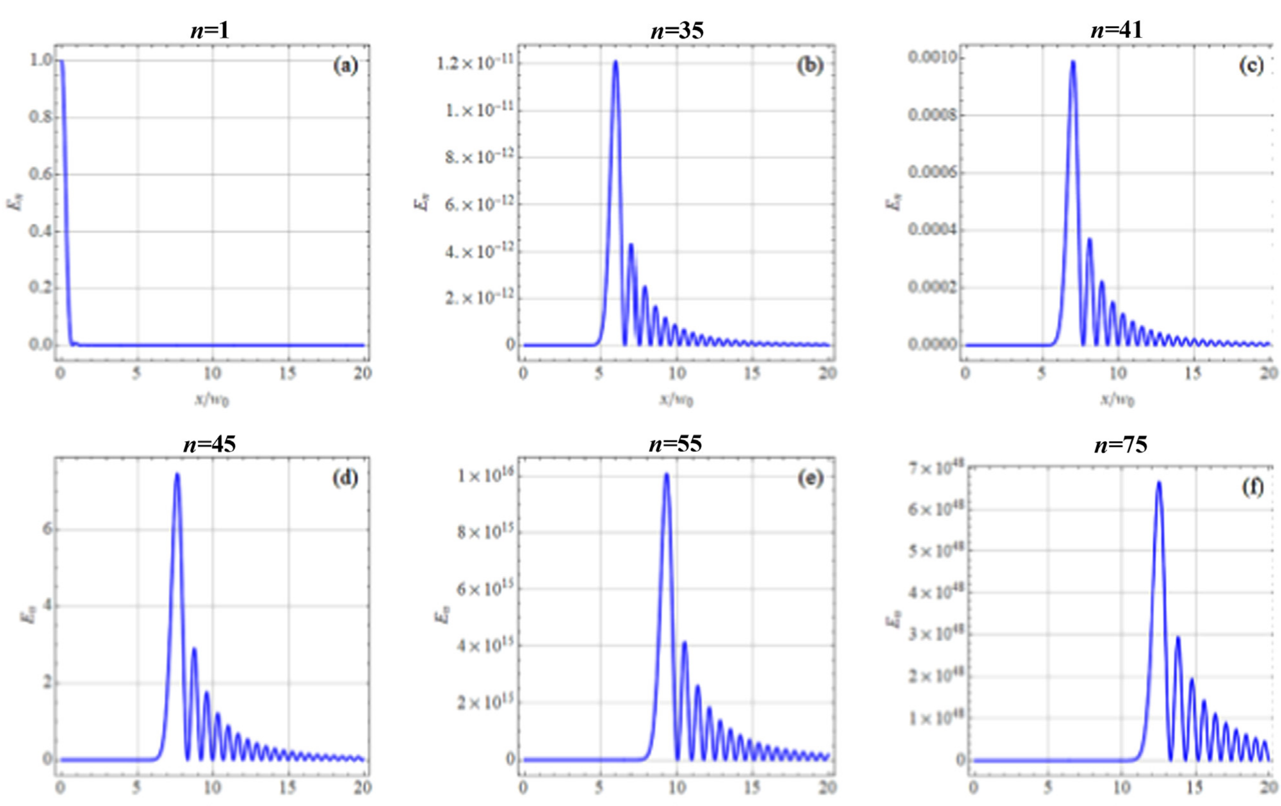

Fig. 9. E_n versus x, for different values of n.

6. Complementary discussion

This section is devoted to two complementary issues. For the first one, let us note that localized approximations are valid for on-axis and off-axis cases, although the focus was on on-axis cases in the present paper. Conversely, standard beam expressions are known only for on-axis cases. Off-axis cases can however be obtained from on-axis cases by using addition theorems of vector spherical wave functions under translations of coordinate systems, an approach originally introduced by Doicu and Wriedt [220], see as well Zhang and Han [221]. The most general case, i.e. when the beams are described in a rotated coordinate system in the case of "oblique" illumination is described in [222–228].

The second issue is the fact that the behavior of the diverging series, observed for both the Davis scheme and the improved standard schemes, is reminiscent of asymptotic series in QED, see Dyson [229] for an early notice. Such series are non-convergent series which however provide a correct result if we limit ourselves to a first few terms. A paradigmatic example is the evaluation of the electron g-factor which is a dimensionless magnetic moment. It may be evaluated by a series reading as:

$$g/2 = 1 + C_1\left(\frac{\alpha}{\pi}\right) + C_2\left(\frac{\alpha}{\pi}\right)^2 + C_3\left(\frac{\alpha}{\pi}\right)^3 + \ldots \tag{105}$$

in which α is a small parameter (the fine structure constant) given by $\alpha = 1/137.035\ldots$ [230], from which we might have expected a fast convergence of the series of Eq. (105). Such is not the case however, and the calculation of the successive coefficients, relying on the evaluation of an increasing number of integrals related to Feynman diagrams, becomes more and more complicated. For instance, the calculation of C_3 requires the calculation of 72 integrals while C_4 requires the evaluation of 891 integrals [231]. In [232], the theoretical value is found to be $g/2 = 1.001\ 159\ 652\ 181\ 13\ (84)$ to be compared with an experimental value given by 1.001 159 652 180 73 (28) according to Hanneke et al. [230]. In such approaches, correct results are obtained by dismissing an infinite number of non-converging terms which is the case we have observed in the present paper, for the Davis scheme where the third-order Davis-Barton beam already provides a satisfactory description of Gaussian beams although the series itself is eventually diverging, and for the improved standard beam as well as illustrated in Fig. 10.

7. Conclusion

The overlooked discovery that the Davis scheme of approximations to the description of Gaussian beams is actually a divergent scheme [179] has been the motivation of the present paper. Two schemes have been nevertheless extracted from the Davis scheme (i) localized approximations (localized beam models) which do not rely on the evaluation of series and are therefore trivially convergent and (ii) the improved standard scheme. The fields in this latter scheme are evaluated by using infinite series and, as for the Davis scheme, it has been for a long time believed that this scheme would be convergent. It has however been found that it is divergent as well, with a critical value n_c in the summations to the evaluation of the fields being the same as in the Davis scheme. The situation encountered in the divergent Davis scheme and in the divergent improved standard scheme is reminiscent of the problem of infinities in QED. In the last case, solutions have been proposed in the framework of superstring theories and, even if superstring theories are still not convincing enough in the mind of some researchers, they provide at least solutions to the physical understanding of the origin of the divergences. In contrast, it is not known whether the infinities encountered in the present paper are purely "accidental" or whether they are a clue for a deeper understanding.

Funding

L.A. Ambrosio acknowledges the partial financial support of the Council for Scientific and Technological Development (CNPq) (426990/2018-8, 309201/2021-7) and of The São Paulo Research Foundation (FAPESP) (2021/06121-0,2020/05280-5).

Declaration of Competing Interest

No conflict of interest.

CRediT authorship contribution statement

Gérard Gouesbet: Conceptualization, Methodology, Formal analysis, Writing – original draft. **Jianqi Shen:** Conceptualization, Methodology, Formal analysis, Writing – review & editing. **Leonardo A. Ambrosio:** Writing – review & editing.

Data availability

No data was used for the research described in the article.

References

[1] Gouesbet G, Gréhan G, Maheu B. Scattering of a Gaussian beam by a Mie scatter center, using a Bromwich formalism. J. Opt. 1985;16(2):83–93. Republished in selected papers on light scattering SPIE Milestone series, Vol 951, 1988, edited by M. Kerker

[2] Gouesbet G, Maheu B, Gréhan G. The order of approximation in a theory of the scattering of a Gaussian beam by a Mie scatter center. J. Opt. 1985;16(5):239–47. Republished in selected papers on light scattering, SPIE Milestone series, Vol. 951, 1988, edited by M. Kerker

[3] Gouesbet G, Gréhan G, Maheu B. Combustion measurements: edited by N. Chigier. New-York, USA: Hemisphere Publishing Corporation; 1991. p. 339–84. chap: Generalized Lorenz-Mie theory and applications to optical sizing

[4] Gouesbet G, Gréhan G. Generalized Lorenz-Mie theories, second edition. Springer International Publishing AG; 2017.

[5] Waterman P. Symmetry, unitarity, and geometry in electromagnetic scattering. Phys Rev D 1971;3(4):825–39.

[6] Mishchenko M, Travis L, Lacis A. Scattering, absorption, and emission of light by small particles. Cambridge University Press, Cambridge; 2002.

[7] Light scattering by nonspherical particles. theory, measurements and applications. Mishchenko M, Hovenier J, Travis L, editors. San Diego: Academic Press; 2000.

[8] Mishchenko M. Electromagnetic scattering by particles and particle groups, an introduction. Cambridge, UK: Cambridge University Press; 2014.

[9] Gouesbet G, Gréhan G. Generalized Lorenz-Mie theories, from past to future. Atomization Sprays 2000;10(3–5):277–333.

[10] Gouesbet G. Generalized Lorenz-Mie theories, the third decade: a perspective. J Quant Spectrosc RadiatTransf 2009;110:1223–38. Invited Review Paper Special issue, XIth conference on Electromagnetic and Light Scattering by Nonspherical Particles (2008)

[11] Gouesbet G. Latest achievements in generalized Lorenz-Mie theories: a commented reference database. Ann Phys 2014;526(11–12):461–89.

[12] Gouesbet G. T-matrix methods for electromagnetic structured beams: a commented reference database for the period 2014–2018. J Quant Spectrosc Radiat Transf 2019;230:247–81.

[13] Kim J, Lee S. Scattering of laser beam and the optical potential well for a homogeneous sphere. J Opt Soc Am 1983;73:303–12.

[14] Gouesbet G, Maheu B, Gréhan G. Scattering of a Gaussian beam by a sphere using a Bromwich formulation: case of an arbitrary location. J Particle Particle Charact 1988;5(1):1–8.

[15] Corbin F, Gréhan G, Gouesbet G. Interaction between a sphere and a Gaussian beam: computations on a micro-computer. J Particle Particle SystCharact 1988;5(3):103–8.

[16] Lock J, Hovenac E. Diffraction of a Gaussian beam by a spherical obstacle. Am J Phys 1993;8:698–707.

[17] Khaled E, Hill S, Barber P. Scattered and internal intensity of a sphere illuminated with a Gaussian beam. IEEE Trans Antennas Propag 1993;41(3):295–303.

[18] Khaled E, Hill S, Barber P. Internal electric energy in a spherical particle illuminated with a plane wave or off-axis Gaussian beam. Appl Opt 1994;33(3):524–32.

[19] Hodges J, Gréhan G, Gouesbet G, Presser C. Forward scattering of a Gaussian beam by a nonabsorbing sphere. Appl Opt 1995;34(12):2120–32.

[20] Lock J, Hodges J. Far-field scattering of a non-Gaussian off-axis axisymmetric laser beam by a spherical particle. Appl Opt 1996;35(33):6605–16.

[21] Barton J. Electromagnetic-field calculations for a sphere illuminated by a higher-order Gaussian beam. I. Internal and near-field effects. Appl Opt 1997;36(6):1303–11.

[22] Barton J. Electromagnetic field calculations for a sphere illuminated by a higher-order Gaussian beam. II Far-field scattering. Appl Opt 1998;37(15):3339–44.
[23] Méés L, Gouesbet G, Gréhan G. Scattering of laser pulses (plane wave and focused Gaussian beams) by spheres. Appl Opt 2001;40(15):2546–50.
[24] Xu F, Ren K, Cai X. Extension of geometrical-optics approximation to on-axis Gaussian beam scattering. I. By a spherical particle. Appl Opt 2006;45(20):4990–9.
[25] Cheng X, Wang X. Wavelength-dependent intensity distribution of a Gaussian beam scattered by a spherical particle. Optik 2010;121:1342–6.
[26] Lock JA, Laven P. Co-polarized and cross-polarized scattering of an off-axis focused Gaussian beam by a spherical particle. 1. Exact GLMT formalism. J Quant Spectrosc RadiatTransf 2018;221:260–72. LIP2018 special issue
[27] Lock JA, Laven P. Co-polarized and cross-polarized scattering of an off-axis focused Gaussian beam by a spherical particle. 2. Sum over azimuthal modes. J Quant Spectrosc RadiatTransf 2018;221:273–85. LIP2018 special issue
[28] Laven P, Lock JA. Co-polarized and cross-polarized scattering of an off-axis focused Gaussian beam by a spherical particle. 3. Diffraction, the Debye series. J Quant Spectrosc RadiatTransf 2018;221:286–99. LIP2018 special issue
[29] Bredikhin V. Gaussian beam sphere optics in condensed matter research. Opt Commun 2020;455. Article 124476
[30] Onofri F, Gréhan G, Gouesbet G. Electromagnetic scattering from a multilayered sphere located in an arbitrary beam. Appl Opt 1995;34(30):7113–24.
[31] Khaled E, Hill S, Barber P. Light scattering by a coated sphere illuminated with a Gaussian beam. Appl Opt 1994;33(15):3308–14.
[32] Sakurai H, Kozaki S. Scattering of a Gaussian beam by a radially inhomogeneous dielectric sphere. J Electromagn Waves Appl 2001;15(12):1673–93.
[33] Li R, Han X, Shi L, Ren K, Jiang H. Debye series for Gaussian beam scattering by a multilayered sphere. Appl Opt 2007;46(21):4804–12.
[34] Li H, Wu Z. Electromagnetic scattering by multilayered spheres in a 2-D Gaussian beaam. Acta Physica Sinica 2008;57(2):833–8.
[35] Yuan Q, et ZJ Li ZW. Electromagnetic scattering for a uniaxial anisotropic sphere in an off-axis obliquely incident Gaussian beam. J Opt Soc Am A 2010;27(6):1457–65.
[36] Wu Z, Li Z, Li H, Yuan Q, Li H. Off-axis Gaussian beam scattering by an anisotropic coated sphere. IEEE Trans Antennas Propag 2011;59(12):4740–8.
[37] Wang M, Zhang H, Liu G, Li Y. Gaussian beam scattering by a rotationally uniaxial anisotropic sphere. J Opt Soc Am A 2012;29(11):2376–80.
[38] Zhang H, Huang Z, Shi Y. Internal and near-surface electromagnetic fields for a uniaxial anisotropic cylinder illuminated with a Gaussian beam. Opt Express 2013;21(13):15645–53.
[39] Chen Z, Zhang H, Huang Z, Wu X. Scattering of on-axis Gaussian beam by a uniaxial anisotropic object. J Opt Soc Am A 2014;31(11):2545–50.
[40] Chen Z, Zhang H, Wu X, Huang Z. Gaussian beam scattering by a gyrotropic anisotropic object. J Quant Spectrosc Radiat Transf 2016;180:1–6.
[41] Zhu X, Liao T, Zhang H, Hui R. Gaussian beam scattering by a chiral sphere. J Quant Spectrosc RadiatTransf 2012;113:1946–50.
[42] Zheng M, Zhang H, Sun Y, Wang Z. Scattering of on-axis Gaussian beam by an arbitrarily shaped chiral object. J Quant Spectrosc Radiat Transf 2015;151:192–7.
[43] Gouesbet G, Gréhan G. Interaction between shaped beams and an infinite cylinder, including a discussion of Gaussian beams. Part Part Syst Char 1994;11:299–308.
[44] Gouesbet G, Gréhan G. Interaction between a Gaussian beam and an infinite cylinder with the use of non-sigma-separable potentials. J Opt Soc Am A 1994;11(12):3261–73.
[45] Gouesbet G. Interaction between Gaussian beams and infinite cylinders, by using the theory of distributions. J. Opt. 1995;26(5):225–39.
[46] Gouesbet G. Scattering of a first-order Gaussian beam by an infinite cylinder with arbitrary location and arbitrary orientation. Part Part Syst Char 1995;12:242–56.
[47] Gouesbet G. Scattering of higher-order Gaussian beams by an infinite cylinder. J Opt 1997;28:45–65.
[48] Ren K, Gréhan G, Gouesbet G. Scattering of a Gaussian beam by an infinite cylinder in the framework of a GLMT, formulation and numerical results. J Opt Soc Am A 1997;14(11):3014–25.
[49] Lock J. Scattering of a diagonally incident focused Gaussian beam by an infinitely long homogeneous circular cylinder. J Opt Soc Am A 1997;14(3):640–52.
[50] Méés L, Ren K, Gréhan G, Gouesbet G. Scattering of a Gaussian beam by an infinite cylinder with arbitrary location and arbitrary orientation: numerical results. Appl Opt 1999;38(9):1867–76.
[51] Gouesbet G, Ren K, Méés L, Gréhan G. Cylindrical localized approximation to speed up computations for Gaussian beams in the generalized Lorenz-Mie theory for cylinders, with arbitrary location and orientation of the scatterer. Appl Opt 1999;38(12):2647–65.
[52] Mroczka J, Wysoczanski D. Plane-wave and Gaussian-beam scattering on an infinite cylinder. Opt Eng 2000;39(3):763–70.
[53] Lock J, Adler C, Hovenac E. Exterior caustics produced in scattering of a diagonally incident plane wave by a circular cylinder : semiclassical scattering theory analysis. J Opt Soc Am A 2000;17(10):1846–56.
[54] Venkatapathi M, Hirleman E. Effect of beam size parameters on internal fields in an infinite cylinder irradiated by an elliptical Gaussian beam. J Opt Soc Am A 2007;24(10):3366–70.
[55] Wang Y, Guo L, Wu Z. Electromagnetic scattering of plane wave/Gaussian beam by parallel cylinders. Acta Physica Sinica 2007;56(1):186–94.
[56] Wu Z, Li H. Debye series of scattering by a multi-layered cylinder in an off-axis 2D Gaussian beam. Chin Phys Lett 2008;25(5):1672–5.
[57] den Bulcke SV, Zhang L, Franchois A, Geffrin J, Stiens J. Plane wave and Gaussian beam scattering by long dielectric cylinders: 2.5D simulations versus measurements. Int J Infrared Millimeter Waves 2008;29(11):1038–47.
[58] Sun X, Wang H, Zhang H. Scattering by an infinite cylinder arbitrarily illuminated with a couple of Gaussian beams. J Electromagn Waves Appl 2010;24(10):1329–39.
[59] Zhai Y, Zhang H, Sun Y. On-axis Gaussian beam scattering by a chiral cylinder. J Opt Soc Am A 2012;29(11):2509–13.
[60] Yang H, Kong P, Yang H-M, Xing S, Zheng G. The far field scattering of single walled nanotubes illuminated by a Gaussian beam. Optik 2013;124:3269–72.
[61] Chen Z, Zhang H, Wu X, Huang Z. Transmission of a Gaussian beam through a gyrotropic cylinder. J Opt Soc Am A 2014;31(9):1931–5.
[62] Yan B, Liu C, Zhang H, Shi Y. Transmission of Gaussian beam through a coated chiral cylinder. Opt Commun 2015;338:261–4.
[63] Chen Z, Zhang H, Wu X. Gaussian beam propagation through a biaxial anisotropic circular cylinder. Optik 2020;223. Article 165650
[64] Gouesbet G, Méés L, Gréhan G. Partial wave expansions of higher-order Gaussian beams in elliptical cylindrical coordinates. J Opt A Pure Appl Opt 1999;1:121–32.
[65] Gouesbet G, Mees L, Gréhan G, Ren K. Localized approximation for Gaussian beams in elliptical cylinder coordinates. Appl Opt 2000;39(6):1008–25.
[66] Han Y, Wu Z. The expansion coefficients of a spheroidal particle illuminated by Gaussian beam. IEEE Trans Antennas Propag 2001;49(4):615–20.
[67] Han Y, Wu Z. Scattering of a spheroidal particle illuminated by a Gaussian beam. Appl Opt 2001;40(15):2501–9.
[68] Han Y, Gréhan G, Gouesbet G. Generalized Lorenz-Mie theory for a spheroidal particle with off-axis Gaussian beam illumination. Appl Opt 2003;42(33):6621–9.
[69] Zhang H, Han Y. Scattering by a confocal multilayered spheroidal particle illuminated by an axial Gaussian beam. IEEE Trans Antennas Propag 2005;53(4):1514–18.
[70] Xu F, Ren K, Cai X, Shen J. Extension of geometrical-optics approximation to on-axis Gaussian beam scattering. II. By a spheroidal particle with end-on incidence. Appl Opt 2006;45(20):5000–9.
[71] Wang H, Sun X, Zhang H. Scattering by a spheroidal particle illuminated by a couple of on-axis Gaussian beams. Opt Laser Technol 2012;44(5):1290–1293.
[72] Han L, Han Y, Wang J, Gouesbet G. Internal and near-surface field distributions for a spheroidal particle illuminated by a focused Gaussian beam: on-axis case. J Quant Spectrosc Radiat Transf 2013;126:38–43.
[73] Sun X, Wang H. Scattering of on-axis polarized Gaussian light beam by spheroidal water coating aerosol particle. Chinese Opt Lett 2014;12(1). Article 012901
[74] Zhao W, Han Y, Han L. Scattering of an oblique incident focused Gaussian beam by a spheroidal particle. J Quant Spectrosc RadiatTransf 2014;145:88–94.
[75] Sun X, Xiao S, Ma L, Su B. Scattering of polarized Gaussian light by a spheroidal particle. Opt Commun 2015;336:24–9.
[76] Tang H, Zheng W. Modeling of scattering intensity of spheroid particles with a Gaussian beam. IOP Conf Ser Earth Environ Sci 2017;61. paper 012133
[77] Gouesbet G, Gréhan G. Generalized Lorenz-Mie theory for assemblies of spheres and aggregates. J Opt A 1999;1(6):706–12.
[78] Bai L, Wu Z, Zhang M, Ren K, Gréhan G. Scattering of cluster spheres located on axis by a Gaussian beam in millimeter waves. Int J Infrared Millimeter Waves 2004;25(8):1221–30.
[79] Bai L, Wu Z, Chen H, Guo L. Scattering of fundamental Gaussian beam from on-axis cluster spheres. Acta Physica Sinica 2005;54(5):2025–9.
[80] Cui Z, Han Y, Zhao W. Scattering of arbitrarily incident Gaussian beams by fractal soot aggregates. J Opt 2012;14. Paper 035703 (10 pp)
[81] Cui Z, Han Y, Wang J, Zhao W. Scattering of Gaussian beam by arbitrarily shaped inhomogeneous particles. J Quant Spectrosc Radiat Transf 2012;113:480–8.
[82] Tang H, Lin J. Scattering of randomly distributed spherical particles illuminated with a Gaussian beam. Laser Phys Lett 2015;12(4). Article 046001
[83] Gouesbet G, Gréhan G. Generalized Lorenz-Mie theory for a sphere with an eccentrically located spherical inclusion. J Mod Opt 2000;47(5):821–37.
[84] Yan B, Zhang H, Liu C. Gaussian beam scattering by a spheroidal particle with an embedded conducting sphere. J Infrared Millimeter Terahertz Waves 2011;32(1):126–33.
[85] Zhai Y, Sun Y, Zhang H. On-axis Gaussian beam scattering by an eccentrically coated conducting cylinder. J. Quant Spectrosc RadiatTransf 2012;113:1441–5.
[86] Han Y, Cui Z, Zhao W. Scattering of Gaussian beam by arbitrarily shaped particles with multiple internal inclusions. Opt Express 2012;20(2):718–31.
[87] Sun X, Zhang H, Wang H, Shen J. On-axis Gaussian beam scattering by a spheroid with a rotationally uniaxial anisotropic spherical inclusion. Opt Laser Technol 2013;45:185–9.
[88] Zheng M, Zhang H, Sun Y. On-axis Gaussian beam scattering by an object with a chiral inclusion. J Quant Spectrosc Radiat Transf 2015;151:269–74.
[89] Zhang H, Chen K, Huang Z, Wang M. Gaussian beam scattering by an infinite cylinder with a spherical inclusion. J Quant Spectrosc RadiatTransf 2020;245. Article 106866
[90] Wang M, Zhang H, Liu G, Li Y, Dong Q. Reflection and transmission of Gaussian beam by a uniaxial anisotropic slab. Opt Express 2014;22(3):3705–11.

[91] Huang Z, Xu F, Wang B, Li M, Zhang H. Propagation of Gaussian beam through a uniaxial anisotropic slab. Opt Commun 2016;380:336–41.
[92] Zhang H, Zhu D, Wang M, Li M, Liao T. Transmission of electromagnetic beam through a uniaxial anisotropic slab. J Quant Spectrosc RadiatTransf 2019;224:114–19. LIP2018 special issue
[93] Zhang H, Yuan Y, Li M, Huang Z. Gaussian beam scattering by a particle above a plane surface. J Quant Spectrosc Radiat Transf 2018;217:22–8.
[94] Han Y, Cui Z, Gouesbet G. Numerical simulation of Gaussian beam scattering by complex particles of arbitrary shape and structure. J Quant Spectrosc Radiat Transf 2012;113(13):1719–27.
[95] Cui Z, Han Y. A review of the numerical investigation on the scattering of Gaussian beam by complex particles. Phys Rep. 2014;538(2):39–75.
[96] Qiu J, Shen J. Beam shape coefficient calculation for a Gaussian beam: localized approximation, quadrature and angular spectrum decomposition methods. Appl Opt 2018;57(2):302–13.
[97] Lock J. Improved Gaussian beam-scattering algorithm. Appl Opt 1995;34(3):559–70.
[98] Moore N, Alonso M. Closed form formula for Mie scattering of nonparaxial analogues of Gaussian beams. Opt Express 2008;16(8):5926–33.
[99] Lock J. Beam shape coefficients of the most general focused Gaussian laser beam for light scattering applications. J Quant Spectrosc Radiat Transf 2013;126:16–24.
[100] Wu P, Han Y, Liu D. Computation of Gaussian beam scattering for larger particles. Acta Physica Sinica 2005;54(6):2676–9.
[101] Sakurai H, Kozaki S. Scattering of a Gaussian beam by stepped index Luneberg lens. Int J Infrared Millimeter Waves 2001;22(11):1653–68.
[102] Wang Y, Guo L, Wu Q. Electromagnetic scattering from two parallel 2D targets arbitrarily located in a Gaussian beam. Chin Phys 2006;15(8):1755–65.
[103] Wang Y, Guo L, Wu Z. Electromagnetic scattering of Gaussian beam by two-dimensional targets. Radio Sci 2007;42(4). Art RS4012
[104] Ashkin A. Optical trapping and manipulations of neutral particles using lasers: a reprint volume with commentaries. Singapore: World Scientific; 2006.
[105] Gouesbet G. Generalized Lorenz-Mie theories and mechanical effects of laser light, on the occasion of Arthur Ashkin's receipt ot the 2018 Nobel prize in physics for his pioneering work in optical levitation and manipulation: a review. J Quant Spectrosc Radiat Transf 2019;225:258–77.
[106] Ren K, Gréhan G, Gouesbet G. Radiation pressure forces exerted on a particle arbitrarily located in a Gaussian beam by using the generalized Lorenz-Mie theory, and associated resonance effects. Opt Commun 1994;108(4–6):343–54.
[107] Zemanek P, Jonas A, Liska M. Simplified description of optical forces acting on a nanoparticle in the Gaussian standing wave. J Opt Soc Am A 2002;19(5):1025–34.
[108] Han Y, Du Y, Zhang H. Radiation trapping forces acting on a two-layered spherical particle in a Gaussian beam. Acta Physica Sinica 2006;55(9):4557–62.
[109] Kotlyar V, Nalimov A. Analytical expression for radiation forces on a dielectric cylinder illuminated by a cylindrical Gaussian beam. Opt Express 2006;14(13):6316–21.
[110] Kotlyar V, Nalimov A. Calculating the pressure force of the non-paraxial cylindrical Gaussian beam exerted upon a homogeneous circular-shaped cylinder. J Mod Opt 2006;53(13):1829–44.
[111] Li Z, Kall M, Xu H. Optical forces on interacting plasmonic nanoparticles in a focused Gaussian beam. Phys Rev B 2008;77(8). Article 085412
[112] Ju W, Yao J, Ding H-P, Wu D-J. Optical radiation forces of focused Gaussian beams on the three-layered microgel particles with near-infrared responses. Appl Phys A 2019;125(82):5pages.
[113] Polaert H, Gréhan G, Gouesbet G. Forces and torques exerted on a multilayered spherical particle by a focused Gaussian beam. Opt Commun 1998;155(1–3):169–79.
[114] Neves A, Camposeo A, Pagliara S, Saija R, Borghese F, Denti P, et al. Rotational dynamics of optically trapped nanofibers. Opt Express 2010;18(2):822–30.
[115] Ambrosio L, Hernandez-Figueroa H. Spin angular momentum transfer from TEM00 focused Gaussian beams to negative refractive index spherical particles. Biomed Opt Express 2011;2(8):2354–63.
[116] Du Y, Han Y, Han G, Li J. Theoretical study on the rotation of particles driven by Gaussian beam. Acta Physica Sinica 2011;60(2). Article number: 028702
[117] Li Z, Wu Z, Shang Q, Bai L, Cao C. Calculation of radiation force and torque exerted on a uniaxial anisotropic sphere by an incident Gaussian beam with arbitrary propagation and polarization directions. Opt Express 2012;20(15):16421–35.
[118] Shang Q, Wu Z, Qu T, Li Z, Bai L, Gong L. Analysis of the radiation force and torque exerted on a chiral sphere by a Gaussian beam. Opt Express 2013;21(7):8677–88.
[119] Mitri F. Radiation force and torque on an elliptical cylinder illuminated by a TE-polarized non-paraxial focused Gaussian light sheet with arbitrary incidence. J Opt Soc Am A 2020;37(2):265–75.
[120] Angelova M, Pouligny B. Trapping and levitation of a dielectric sphere with off-axis centered Gaussian beams. I. Experimental. Pure Appl Opt 1993;2:261–76.
[121] Martinot-Lagarde G, Pouligny B, Angelova M, Gréhan G, Gouesbet G. Trapping and levitation of a dielectric sphere with off-centred Gaussian beams. II. GLMT-analysis. Pure Appl Opt 1995;4(5):571–85.
[122] Bayoudh S, Nieminen T, Heckenberg N, Rubinsztein-Dunlop H. Orientation of biological cells using plane-polarized Gaussian beam optical tweezers. J Mod Opt 2003;50(10):1581–90.
[123] Simpson S, Hanna S. Optical trapping of spheroidal particles in Gaussian beams. J Opt Soc Am A 2007;24(2):430–43.
[124] Ambrosio L, Hernandez-Figueroa H. Fundamentals of negative refractive index optical trapping: forces and radiation pressures exerted by focused Gaussian beams using the generalized Lorenz-Mie theory. Biomed Opt Express 2010;1(5):1284–301.
[125] Chang C, Huang W-X, Lee K, Sung H. Optical levitation of a non-spherical particle in a loosely focused Gaussian beam. Opt Express 2012;20(21):24068–84.
[126] Bareil P, Sheng Y. Modeling highly focused laser beam in optical tweezers with the vector Gaussian beam in the T-matrix method. J Opt Soc Am A 2013;30(1):1–6.
[127] Mitri F. Optical trapping of a perfect electromagnetic conductor (PEMC) sphere exhibiting rotary polarization using nonparaxial focused Gaussian single-beam tweezers. Results Opt 2021;4. Article 100089
[128] Chen J, Ng J, Wang P, Lin Z. Analytical partial wave expansion of vector Bessel beam and its application to optical binding. Opt Lett 2010;35(10):1674–6.
[129] Bai J, Wu Z, Ge C, Shang Q, Li Z, Gong L. Analysis of lateral binding force exerted on multilayered spheres induced by high-order Bessel beams with arbitrary polarization angles. J Quant Spectrosc RadiatTransf 2018;221:183–93. LIP2018 special issue
[130] Chen Y-F, Blab G, Meiners J-C. Stretching submicron biomolecules with constant-force axial optical tweezers. Biophys J 2009;96:4701–8.
[131] Xu F, Lock J, Gouesbet G, Tropea C. Optical stress on the surface of a particle. I. Homogeneous sphere. Phys Rev A 2009;79. Article number: 053808
[132] Yeh Y, Cummins H. Localized fluid flow measurements with a He-Ne laser spectrometer. Appl Phys Lett 1964;4(10):176–8.
[133] Gréhan G, Gouesbet G, Naqwi A, Durst F. Particle trajectory effects in phase-Doppler systems: computations and experiments. Part Part Syst Char 1993;10(6):332–8.
[134] Gréhan G, Gouesbet G, Naqwi A, Durst F. Trajectory ambiguities in phase–Doppler systems: study of a near-forward and a near-backward geometry. Part Part Syst Char 1994;11(2):133–44.
[135] Onofri F, Blondel D, Gréhan G, Gouesbet G. On the optical diagnosis and sizing of spherical coated and multilayered particles with phase-Doppler anemometry. Part Part Syst Char 1996;13(2):104–11.
[136] Onofri F, Girasole T, Gréhan G, Gouesbet G, Brenn G, Domnick J, et al. Phase–Doppler anemometry with the dual burst technique for measurement of refractive index and absorption coefficient simultaneously with size and velocity. Part Part Syst Char 1996;13(2):112–24.
[137] Selmke M, Braun M, Cichos F. Gaussian beam photothermal single particle microscopy. J Opt Soc Am A 2012;29(10):2237–41.
[138] Lock J. Contribution of high-order rainbows to the scattering of a Gaussian laser beam by a spherical particle. J Opt Soc Am A 1993;10(4):693–706.
[139] Lock J, Adler C. Debye-series analysis of the first-order rainbow produced in scattering of a diagonally incident plane wave by a circular cylinder. J Opt Soc Am A 1997;14:1316–28.
[140] Guo L, Wu Z. Rainbow scattering by an inhomogeneous cylinder with an off-axis Gaussian beam incidence at normal. Int J I 2000;21(11):1038–47.
[141] Saengkaew S, Charinpanitkul T, Vanisri H, Tanthapanichakoon W, Mééš L, Gouesbet G, et al. Rainbow refractometry: on the validity domain of Airy's and Nussenzweig's theories. Opt Commun 2006;259:7–13.
[142] Saengkaew S, Charinpanikul T, Laurent C, Biscos Y, Lavergne G, Gouesbet G, et al. Processing of individual rainbow signals. Exp Fluids 2010;48:111–19.
[143] Yu H, Sun H, Shen J, Tropea C. Measurement of refractive index and size of a spherical drop from Gaussian beam scattering in the primary rainbow region. J Quant Spectrosc Radiat Transf 2018;207:83–8.
[144] Cao Y, Wang W, Yu H, Shen J, Tropea C. Characterization of refractive index and size of a spherical drop by using Gaussian beam scattering in the secondary rainbow region. J Quant Spectrosc Radiat Transf 2020;242. Article 106785
[145] Wang J, Yu H, Shen J, Yang B, Tropea C. Simulation of the optical caustics associated with the primary rainbow for oblate spheroidal drops illuminated by a Gaussian beam. Opt Express 2021;29(1):377–84. Article 106785
[146] Nicolas E, Coëtmellec S, Brunel M, Allano D, Lebrun D, Janssen A. Application of the fractional Fourier transformation to digital holography recorded by an elliptical and astigmatic Gaussian beam. J Opt Soc Am A 2005;22:2569–2577.
[147] Rémacha C, Coëtmellec S, Brunel M, Lebrun D. Extended wavelet transformation to digital holographic reconstruction: application to the elliptical, astigmatic Gaussian beams. Appl Opt 2013;52:838–48.
[148] Lock J. Interpretation of extinction in Gaussian-beam scattering. J Opt Soc Am A 1995;12(5):929–38.
[149] Shen J, Riebel U. Extinction by a large spherical particle located in a narrow Gaussian beam. Part Part Syst Char 2002;18(5–6):254–61.
[150] Bosch S, Sancho-Parramon J. Procedures for the measurement of the extinction cross section of one particle using a Gaussian beam. J Quant Spectrosc Radiat Transf 2016;180:77–83.
[151] Castagner J, Jones A. A double Gaussian beam method for the determination of particle size, direction and velocity. Part Part Syst Char 2004;21(1):5–14.
[152] Khaled E, Hill S, Barber P, Chowdhury D. Near-resonance excitation of dielectric spheres with plane waves and off-axis Gaussian beams. Appl Opt 1992;31(9):1166–9.

[153] Lock J. Morphology-dependent resonances of an infinitely long circular cylinder illuminated by a diagonally incident plane wave or a focused Gaussian beam. J Opt Soc Am A 1997;14(3):653–61.

[154] Lock J. Excitation efficiency of a morphology-dependent resonance by a focused Gaussian beam. J Opt Soc Am A 1998;15(12):2986–94.

[155] Poon A, Chang R, Lock J. Spiral morphology-dependent resonances in an optical fiber: effects of fiber tilt and focused Gaussian beam illumination. Opt Lett 1998;23(14):1105–7.

[156] Wang J, Gouesbet G, Gréhan G, Saengkaew S. Morphology-dependent resonances in an eccentrically layered sphere illuminated by a tightly focused off-axis Gaussian beam. J Opt Soc Am A 2011;28(9):1849–59.

[157] Han L, Han Y, Gouesbet G, Wang J, Gréhan G. Photonic jet generated by spheroidal particle with Gaussian-beam illumination. J Opt Soc Am B 2014;31(7):1476–83.

[158] Uenohara T, Mizutani Y, Takaya Y. Comparison of intensity distribution of photonic nanojet according to Gaussian beam and radially polarization beam incidence. Precis Eng 2019;60:274–9.

[159] Mandal A, Dantham V. Short and elongated photonic nanojets emerged from single solid/hollow core-shell microparticles illuminated by focused Gaussian beams and plane wave. J Quant Spectrosc RadiatTransf 2020;257. Article 107350

[160] Lock J, Hodges J, Gouesbet G. Failure of the optical theorem for Gaussian-beam scattering by a spherical particle. J Opt Soc Am A 1995;12(12):2708–15.

[161] Gouesbet G, Letellier C, Gréhan G, Hodges J. Generalized optical theorem for on-axis Gaussian beams. Opt Commun 1996;125:137–57.

[162] Davis L. Theory of electromagnetic beams. Phys Rev 1979;19(3):1177–9.

[163] Cui Z, Han Y, Zhang H. Scattering of an arbitrarily incident focused Gaussian beam by arbitrarily shaped dielectric particles. J Opt Soc Am B 2011;28(11):2625–32.

[164] Li J, Wu X. FDTD simulation of trapping nanowires with linearly polarized and radially polarized optical tweezers. Opt Express 2011;19(21): 20736–20741.

[165] Lock J. Angular spectrum and localized model of Davis-type beam. J Opt Soc Am A 2013;30(3):489–500.

[166] Qin S, Li R, Yang R, Ding C. Debye series analysis of internal and near–surface fields for a homogeneous sphere illuminated by an axicon-generated vector Bessel beam. J Quant Spectrosc Radiat Transf 2017;195:26–34.

[167] Wang J, Wriedt T, Lock J, Mädler L. General description of circularly symmetric Bessel beams of arbitrary order. J Quant Spectrosc Radiat Transf 2016;184:218–32.

[168] Al-Jarro A, Biris C, Panolu N. Resonant mixing of optical orbital and spin angular momentum by using chiral silicon nanosphere clusters. Opt Express 2016;24(7):6945–58.

[169] Jia X, Shen J, Yu H. Calculation of generalized Lorenz-Mie theory based on the localized beam models. J Q 2017;195:44–54.

[170] Wang W, Zhang H, Sun Y. Semi-analytical solution to arbitrarily shaped beam scattering. J Quant Spectrosc Radiat Transf 2017;195:114–18.

[171] Xu K, Pan X-M, Li R, Sheng X-Q. Fast and accurate algorithm for repeated optical trapping simulations on arbitrarily shaped particles based on boundary element method. J Quant Spectrosc Radiat Transf 2017;195:76–84.

[172] Ge C-X, Wu Z-S, Bai J, Gong L. Effect of nanoscale roughness on optical trapping properties of surface plasmon polaritons exerted on nanoparticle. J Quant Spectrosc RadiatTransf 2018;219:339–49. LIP2018 special issue

[173] Chen Z, Zhang H, Wu X, Nian F. Electromagnetic beam propagating through a gyrotropic anisotropic circular cylinder. J Quant Spectrosc RadiatTransf 2021;262. Article 107519, Virtual special of LIP2020

[174] Yan B, Zhang H, Zhang J, Liu C, Lin X. Electromagnetic wave beam propagation through a chiral slab. Chin J Phys 2021;73:613–21.

[175] Gouesbet G. Measurements of beam shape coefficients in generalized Lorenz-Mie theory and the density-matrix approach. I. Measurements. Part Part Syst Char 1997;14:12–20.

[176] Gouesbet G. Measurements of beam shape coefficients in generalized Lorenz-Mie theory and the density-matrix approach. II. The density-matrix approach. Part Part Syst Char 1997;14:88–92.

[177] Polaert H, Gouesbet G, Gréhan G. Measurements of beam shape coefficients in the generalized Lorenz-Mie theory for the on-axis case: numerical simulations. Appl Opt 1998;37(21):5005–13.

[178] Polaert H, Gouesbet G, Gréhan G. Laboratory determination of beam shape coefficients for use in generalized Lorenz-Mie theory. Appl Opt 2001;40(10):1699–706.

[179] Wang G-Z, Webb J. New method to get fundamental Gaussian beam's perturbation solution and its global property. Appl Phys B 2008;93: 345–348.

[180] Barton J, Alexander D. Fifth-order corrected electromagnetic field components for fundamental Gaussian beams. J Appl Phys 1989;66(7):2800–2.

[181] Schaub S, Barton J, Alexander D. Simplified scattering coefficients for a spherical particle located on the propagation axis of a fifth-order Gaussian beam. Appl Phys Lett 1989;55:2709–11.

[182] Gouesbet G, Lock J, Gréhan G. Partial wave representations of laser beams for use in light scattering calculations. Appl Opt 1995;34(12):2133–43.

[183] Lax M, Louisell W, Knight LM. From Maxwell to paraxial optics. Phys Rev A 1975;11(4):1365–70.

[184] Agrawal G, Pattanayak D. Gaussian beam propagation beyond the paraxial approximation. J Opt Soc Am 1979;69(4):575–8.

[185] Seshadri S. Fundamental electromagnetic Gaussian beam beyond the paraxial approximation. J Opt Soc Am A 2008;25(9):2156–64.

[186] Cao N, Ho Y, Kong Q, Wang P, Yuan X, Nishida Y, et al. Accurate description of Gaussian laser beams and electron dynamics. Opt Commun 2002;204:7–15.

[187] Lock J, Gouesbet G. Rigorous justification of the localized approximation to the beam shape coefficients in generalized Lorenz-Mie theory. I. On-axis beams. J Opt Soc Am A 1994;11(9):2503–15.

[188] Gouesbet G, Lock J. Rigorous justification of the localized approximation to the beam shape coefficients in generalized Lorenz-Mie theory. II. Off-axis beams. J Opt Soc Am A 1994;11(9):2516–25.

[189] Gouesbet G. Higher-order descriptions of Gaussian beams. J. Opt. 1996;27(1):35–50.

[190] Kogelnik H. Imaging of optical modes, resonators with internal lenses. Bell Syst Techn J 1965:455–94.

[191] Kogelnik H, Li T. Laser beams and resonators. Proc IEEE 1965;54:1312–29.

[192] Kogelnik H, Li T. Laser beams and resonators. Appl Opt 1966;5(10):1550–6.

[193] Alexopoulos N, Park P. Scattering of waves with normal amplitude distribution from cylinders. IEEE Trans Antennas Propag 1972:216–17.

[194] Gouesbet G, Lock J. Consequences of the angular spectrum decomposition of a focused beam including slower than c beam propagation. J Quant Spectrosc Radiat Transf 2016;178:142–51.

[195] Chen C, Konkola P, Ferrera J, Heilmann R, Schattenburg M. Analyses of vector Gaussian beam propagation and the validity of paraxial and spherical approximations. J Opt Soc Am A 2002;19(2):404–12.

[196] Gouesbet G, Lock J, Han Y, Wang J. Efficient computation of arbitrary beam scattering on a sphere: comments and rebuttal, with a review on the angular spectrum decomposition. J Quant Spectrosc Radiat Transf 2021;276. Article 107913

[197] Gouesbet G, Letellier C, Ren K, Gréhan G. Discussion of two quadrature methods of evaluating beam shape coefficients in generalized Lorenz-Mie theory. Appl Opt 1996;35(9):1537–42.

[198] Gouesbet G, Ambrosio L, Lock J. On an infinite number of quadratures to evaluate beam shape coefficients in generalized Lorenz-Mie theory and extended boundary condition method for structured EM fields. J Quant Spectrosc Radiat Transf 2020;242. Article 196779, 4 pages

[199] Robin L. Fonctions sphériques de Legendre et fonctions sphéroidales, vol 1, 2, 3. Paris: Gauthier-Villars; 1957.

[200] Gouesbet G, Gréhan G. Sur la généralisation de la théorie de Lorenz-Mie. J Opt 1982;13(2):97–103.

[201] Gréhan G, Maheu B, Gouesbet G. Scattering of laser beams by Mie scatter centers: numerical results using a localized approximation. Appl Opt 1986;25(19):3539–48.

[202] Gouesbet G, Maheu B, Gréhan G. Light scattering from a sphere arbitrarily located in a Gaussian beam, using a Bromwich formulation. J Opt Soc Am A 1988;5(9):1427–43.

[203] Polaert H, Gréhan G, Gouesbet G. Improved standard beams with applications to reverse radiation pressure. Appl Opt 1998;37(12):2435–40.

[204] Gouesbet G, Gréhan G, Maheu B. Expressions to compute the coefficients g_n^m in the generalized Lorenz-Mie theory, using finite series. J. Opt. 1988;19(1):35–48.

[205] Gouesbet G, Gréhan G, Maheu B. Computations of the g_n coefficients in the generalized Lorenz-Mie theory using three different methods. Appl Opt 1988;27(23):4874–83.

[206] van de Hulst H. Light scattering by small particles. New York: Wiley; 1957.

[207] Maheu B, Gréhan G, Gouesbet G. Ray localization in Gaussian beams. Opt Commun 1989;70(4):259–62.

[208] Maheu B, Gréhan G, Gouesbet G. Generalized Lorenz-Mie theory: first exact values and comparisons with the localized approximation. Appl Opt 1987;26(1):23–5.

[209] Gouesbet G, Lock J, Gréhan G. Generalized Lorenz-Mie theories and description of electromagnetic arbitrary shaped beams: localized approximations and localized beam models, a review. J Quant Spectrosc Radiat Transf 2011;112:1–27.

[210] Wang J, Gouesbet G. Note on the use of localized beam models for light scattering theories in spherical coordinates. Appl Opt 2012;51(17): 3832–3836.

[211] Gouesbet G. Second modified localized approximation for use in generalized Lorenz-Mie theories and other theories revisited. J Opt Soc Am A 2013;30(4):560–4.

[212] Gouesbet G. On the validity of localized approximations for Bessel beams: all N-Bessel beams are identically equal to zero. J Quant Spectrosc Radiat Transf 2016;176:82–6.

[213] Chafiq A, Ambrosio L, Gouesbet G, Belafhal A. On the validity of the integral localized approximation for on-axis zeroth-order Mathieu beams. J Quant Spectrosc Radiat Transf 2018;204:27–34.

[214] Gouesbet G, Ambrosio L. On the validity of the use of a localized approximation for helical beams. I. Formal aspects. J Quant Spectrosc Radiat Transf 2018;208:12–18.

[215] Ambrosio L, Gouesbet G. On the validity of the use of a localized approximation for helical beams. II. Numerical aspects. J Quant Spectrosc Radiat Transf 2018;215:41–50.

[216] Gouesbet G. Validity of the localized approximation for arbitrary shaped beams in generalized Lorenz-Mie theory for spheres. J Opt Soc Am A 1999;16(7):1641–50.

[217] Gouesbet G, Gréhan G, Maheu B. On the generalized Lorenz-Mie theory: first attempt to design a localized approximation to the computation of the coefficients g_n^m. J. Opt. 1989;20(1):31–43.
[218] Gouesbet G, Gréhan G, Maheu B. Localized interpretation to compute all the coefficients g_n^m in the generalized Lorenz-Mie theory. J Opt Soc Am A 1990;7(6):998–1007.
[219] Ren K, Gréhan G, Gouesbet G. Prediction of reverse radiation pressure by generalized Lorenz-Mie theory. Appl Opt 1996;35(15):2702–10.
[220] Doicu A, Wriedt T. Computation of the beam shape coefficients in the generalized Lorenz-Mie theory by using the translational addition theorem for spherical vector wave functions. Appl Opt 1997;36(13):2971–8.
[221] Zhang H, Han Y. Addition theorem for the spherical vector wave functions and its application to the beam shape coefficients. J Opt Soc Am B 2008;25(2):255–60.
[222] Han Y, Zhang H, Han G. The expansion coefficients of arbitrary shaped beam in oblique illumination. Opt Express 2007;15(2):735–46.
[223] Han Y, Zhang Y, Zhang H, Han G. Scattering of typical particles by beam shape in oblique illumination. J Quant Spectrosc Radiat Transf 2009;110(14–16):1375–81.
[224] Gouesbet G, Wang J, Han Y. Transformations of spherical beam shape coefficients in generalized Lorenz-Mie theories through rotations of coordinate system. I. General formulation. Opt Commun 2010;283(17):3218–25.
[225] Wang J, Gouesbet G, Han Y. Transformations of spherical beam shape coefficients in generalized Lorenz-Mie theories through rotations of coordinate system. II. Axisymmetric beams. Opt Commun 2010;283(17):3226–34.
[226] Gouesbet G, Wang J, Han Y. Transformations of spherical beam shape coefficients in generalized Lorenz-Mie theories through rotations of coordinate system. III. Special values of Euler angles. Opt Commun 2010;283(17):3235–3243.
[227] Gouesbet G, Wang J, Han Y. Transformations of spherical beam shape coefficients in generalized Lorenz-Mie theories through rotations of coordinate system. IV. Plane waves. Opt Commun 2010;283(17):3244–54.
[228] Gouesbet G, Lock J, Wang J, Gréhan G. Transformations of spherical beam shape coefficients in generalized Lorenz-Mie theories through rotations of coordinate system. V. localized beam models. Opt Commun 2011;284(1):411–17.
[229] Dyson F. Divergence of perturbation theory in quantum electrodynamics. Phys Rev 1952;85:631–2.
[230] Hanneke D, Fogwell S, Gabrielse G. New measurement of the electron magnetic moment and the fine structure constant. Phys Rev Lett 2008;100. Article 120801
[231] Gabrielse G, Hanneke D, Kinoshita T, Nio M, Odom B. New determination of the fine structure constant from the electron g value and QED. Phys Rev Lett 2006;97. Article 030802
[232] Bouchendira R, Cladé P, Guellati-Khélifa S, Nez F, Biraben F. New determination of the fine structure constant and test of the quantum electrodynamics. Phys Rev Lett 2011;106. Article 080801